NOTICE

The quality of this microform is heavily dependent upon the quality of the original thesis submitted for microfilming. Every effort has been made to ensure the highest quality of reproduction possible.

If pages are missing, contact the university which granted the degree.

Some pages may have indistinct print especially if the original pages were typed with a poor typewriter ribbon or if the university sent us an inferior photocopy.

Reproduction in full or in part of this microform is governed by the Canadian Copyright Act, R.S.C. 1970, c. C-30, and subsequent amendments.

AVIS

La qualité de cette microforme dépend grandement de la qualité de la thèse soumise au microfilmage. Nous avons tout fait pour assurer une qualité supérieure de reproduction.

S'il manque des pages, veuillez communiquer avec l'université qui a conféré le grade.

La qualité d'impression de certaines pages peut laisser à désirer, surtout si les pages originales ont été dactylographiées à l'aide d'un ruban usé ou si l'université nous a fait parvenir une photocopie de qualité inférieure.

La reproduction, même partielle, de cette microforme est soumise à la Loi canadienne sur le droit d'auteur, SRC 1970, c. C-30, et ses amendements subséquents.

Canadä

UNIVERSITY OF ALBERTA

Shear Wave Velocity Measurement of

Cohesionless Soils for Evaluation of In-Situ State

BY

A THESIS SUBMITTED TO THE FACULTY OF GRADUATE STUDIES AND RESEARCH IN PARTIAL FULFILLMENT OF THE REQUIRMENTS FOR THE DEGREE OF MASTER OF SCIENCE.

IN

GEOTECHNICAL ENGINEERING

DEPARTMENT OF CIVIL ENGINEERING

EDMONTON, ALBERTA

FALL, 1994

National Library of Canada

Acquisitions and
Bibliographic Services Branch

395 Wellington Street
Ottawa, Ontario
K1A 0N4

Bibliothèque nationale du Canada

Direction des acquisitions et
des services bibliographiques

395, rue Wellington
Ottawa (Ontario)
K1A 0N4

The author has granted an irrevocable non-exclusive licence allowing the National Library of Canada to reproduce, loan, distribute or sell copies of his/her thesis by any means and in any form or format, making this thesis available to interested persons.

The author retains ownership of the copyright in his/her thesis. Neither the thesis nor substantial extracts from it may be printed or otherwise reproduced without his/her permission.

L'auteur a accordé une licence irrévocable et non exclusive permettant à la Bibliothèque nationale du Canada de reproduire, prêter, distribuer ou vendre des copies de sa thèse de quelque manière et sous quelque forme que ce soit pour mettre des exemplaires de cette thèse à la disposition des personnes intéressées.

L'auteur conserve la propriété du droit d'auteur qui protège sa thèse. Ni la thèse ni des extraits substantiels de celle-ci ne doivent être imprimés ou autrement reproduits sans son autorisation.
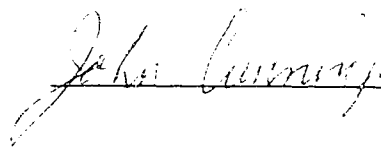
ISBN 0-315-95022-6

Canada

UNIVERSITY OF ALBERTA

RELEASE FORM

NAME OF AUTHOR: **John Cecil Cunning**

TITLE OF THESIS: **Shear Wave Velocity Measurement of Cohesionless Soils for the Evaluation of In-situ State**

DEGREE: **Master of Science**

YEAR THIS DEGREE GRANTED: **1994**
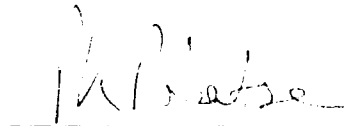
John Cecil Cunning

#304-10504-77th. Ave
Edmonton, AB
T6E 1N1

Date: May 26, 1994
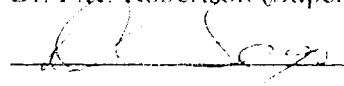
UNIVERSITY OF ALBERTA

FACULTY OF GRADUATE STUDIES AND RESEARCH

The undersigned certify that they have read, and recommend to the Faculty of Graduate Studies and Research for acceptance, a thesis entitled **Shear Wave Velocity Measurement of Cohesionless Soils for the Evaluation of In-situ State** submitted by **John Cecil Cunning** in partial fulfillment of the requirements for the degree of **Master of Science** in **Geotechnical Engineering**.

Dr. P.K. Robertson (Supervisor)

Dr. D.C. Sego (Co-Supervisor)

Dr. D. Chan

Dr. K. Barron

Date: May 16, 1994

ABSTRACT

Shear wave velocity (Vs) measurements were carried out in a triaxial testing program on three cohesionless soil materials. The Vs was measured with bender element technology. The loading head and base pedestal of the triaxial cell were modi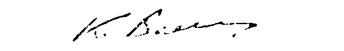fied to incorporate bender elements. The initial system used was a single bender system that protruded 10 mm into the sample (Sasitharan, 1994). As a part of this research a bender element system that was flush mounted in the head and base was developed. Vs was measured both during consolidation and at ultimate steady state. These Vs measurements on three different cohesionless soils were used to develop relationships between the void ratio (e), mean normal effective stress (p') and Vs. After consolidation the soil samples were loaded in shear under constant strain rate triaxial compression either drained or undrained in order to determine their ultimate steady state (USS) at large strains. The results were expressed within the framework of Critical State Soil Mechanics. The results of the Vs and USS information were combined with the state parameter concept in order to use Vs to determine the contractive/dilative boundary with respect to vertical effective stress for large strain loading. Thus Vs could be used as a design aid in determining if a soil deposit was susceptible to flow liquefaction. A suggested flow liquefaction evaluation procedure is given based on the method developed in this research. The results of this method are compared to that of previously existing correlations. Two worked examples of the suggested flow liquefaction evaluation procedure are given.

ACKNOWLEDGEMENTS

TABLE OF CONTENTS

LIST OF TABLES

LIST OF FIGURES

LIST OF NOMENCLATURE

A	intercept of Vs1 - e relationship at e=0
a_{max}	maximum ground acceleration
AP	air pluviated
AS	Alaska sand
ASTM	American Society for Testing and Materials
B	slope of Vs1- e relationship
b	protruding distance of both bender elements
CANLEX	Canadian Liquefaction Experiment
CPT	Cone Penetration Test
CSSM	Critical State Soil Mechanics
CVRL	critical voids ratio line
e	void ratio
G	shear modulus
Go	small strain shear modulus
Gs	specific gravity of the solids
Hcurr	current height of sample
Ko	coefficient of earth pressure at rest
LSS	limited stain softening
LVDT	linear voltage displacement transducer
M	quss/p'uss
M_{PT}	q/p' at the PT
Ms	mass of solids,
MT	moist tamping
m_1	constant
m_2	constant
N	SPT blow count per foot penetration
n	stress exponent
OS	Ottawa sand
Pa	reference pressure, (usually 100 kPa)
p'	mean normal effective stress
p'c	mean normal effective consolidation stress
PT	phase transformation
p'uss	mean normal effective stress at USS

q	deviator stress
qc	CPT tip resistance
QSS	quassi steady state
quss	deviator stress at USS
r^2	regression coefficient measure of fit
RC	Resonant Column
s	the slope of the collapse surface in the stress path plot
SASW	Spectral Analysis of Surface Waves
SCPT	Seismic Cone Penetration Test
SEM	Scanning Electron Microscope
SH	strain hardening
SPT	Standard Penetration Test
SS	Syncrude sand
ss	strain softening
SS/CS	steady state/critical state
Δt	travel time of shear wave
USS	ultimate steady state
USSL	ultimate steady state line
ΔVcons	measured volume change during consolidation
Vinit	initial sample volume
ΔVmem cor	membrane correction in volume due to penetration
Vp	compression wave velocity
Vs	shear wave velocity
ΔVsat	calculated volume change during saturation
Vs1	normalized shear wave velocity
$(Vs)_{\psi=0}$	Vs for zero state parameter
WP	water pluviation
Γ	intercept of the steady state line in e-log p' space at p'=1
ε_a	axial strain
ε_v	volumetric strain
λ	slope of the steady state line in e-log p' space
ρ	soil mass density
ρw	density of water
σ'_a	effective stress in direction of wave propagation
σ'_b	effective stress in direction of particle motion

σ'_c	effective stress in direction perpendicular to a and b
σ'_h	effective stress in horizontal direction
σ'_p	effective stress in perpendicular to axial direction
σ'_v	effective stress in vertical direction
σ'_1	effective stress in major principal direction in triaxial test
σ'_3	effective stress in minor principal direction in triaxial test
ϕ	mobilized friction angle
ϕ_{cv}	constant volume friction angle
Ψ	state parameter

1.0 Introduction

1.1 Purpose of Investigation

Deposits of cohesionless soils can exist in both natural and engineered forms. Geotechnical engineering evaluation for the stability of slopes in these deposits or for foundations of structures on these deposits requires an investigation into the mechanical behaviour for various static and dynamic loading conditions. This evaluation requires a knowledge of the in-situ state of the soil deposit. For any soil deposit the evaluation of in-situ state can be undertaken by either obtaining samples of the soil for laboratory testing, or by performing in-situ tests.

Representative laboratory samples of cohesionless soils are difficult to obtain. Thus the interest is in in-situ testing. Two primary in-situ tests are the Standard Penetration Test (SPT) and the Cone Penetration Test (CPT). Other more advanced in-situ testing involves the measurement of shear wave velocity (Vs), resulting in an interval profile of Vs with depth. There are many empirical correlations to evaluate the potential for liquefaction susceptibility from the SPT blow count (N) (Seed, 1979) or from the CPT tip resistance (qc) (Robertson *et al.*, 1992b). However, there is only limited information on the use of Vs for the evaluation of the liquefaction susceptibility or in-situ state of a soil.

Presently the geotechnical literature shows that the Vs measured in the field can be compared to a historical data base where Vs was measured at sites where liquefaction was or was not reported. A value of Vs < 140 m/s is given by Stokoe and Nazarian (1985) or a normalized shear wave velocity value of (Vs1) < 160 m/s by Robertson (1993) as values below which the potential for liquefaction problems occurring under certain dynamic loading is high. These are empirical approaches which are based more on experience than on engineering theory.

Vs is a small strain measurement related directly to the small strain shear modulus (Go). Two of the most fundamental properties of any engineering material are the shear modulus and the bulk modulus. Much geotechnical information is estimated from the SPT N. It is believed that the factors that effect the N value also affect the in-situ measured Vs value and that the Vs value is more sensitive to the changing factors

(Strachan, 1981; Tokimatsu *et al.*, 1986). Thus it is expected that more geotechnical information about the soil can be interpreted from the Vs.

It is the goal of this research to estimate in-situ soil state from the field measurement of Vs. This can be accomplished through a laboratory developed relationship of the void ratio (e)- the mean normal effective stress (p') - and the Vs. This interpreted in-situ state can, within the framework of critical state soil mechanics (CSSM), be compared to the ultimate steady state (USS). Thus based on the field measured Vs and effective stress condition a prediction about the large strain contractive/dilative behaviour may be made.

1.2 Object of this Research

In order to describe the in-situ physical state of a cohesionless soil one must know the void ratio and the effective stress state relative to the ultimate steady state of the soil From this information an engineering evaluation of the soil profile may proceed.

High quality undisturbed samples of cohesionless soils can be difficult and expensive to obtain. Ground freezing is one method to obtain the highest quality samples available (Sego *et al.*, 1993; Yoshimi *et al.*, 1989). However, due to the expense of obtaining these samples ground freezing tends to be reserved for large budget engineering projects. For the small routine investigations an alternative method of analysis of a soil profile is required.

Laboratory tests may be carried out on reconstituted samples of cohesionless soils However, the choice of preparation method may influence the steady state results (Mulilis *et al.*, 1977). Laboratory testing of reconstituted samples can be carried out in combination with Vs measurements. Vs measurement gives the possibility of regaining the in-situ state by matching the laboratory Vs with the field Vs at the same stress and void ratio conditions so that preparation effects can be neglected.

In-situ tests can be used to estimate the basic properties of a soil deposit. Tests such as the SPT and CPT provide valuable estimates of soil properties but they do not provide physical state information like void ratio and their interpretations often do not fully involve CSSM concepts. Vs measurements can now be routinely undertaken in the

2

field in a soil investigation as well as in the laboratory, hence the interest in shear wave velocity in this research.

This program builds on work initiated at the University of Alberta by Sasitharan (1994). He developed an e-p'-Vs relationship for Ottawa sand with tests carried out in a triaxial testing device modified to incorporate bender elements for the measurement of Vs. The tests were carried out under monotonic triaxial compression, either undrained or drained, on reconstituted samples of clean Ottawa sand. By measuring the shear wave velocity during consolidation and at steady state after shearing, the relationship between the e-p'-Vs was developed.

For this study a series of monotonic triaxial compression, either drained or undrained, with Vs measurement was carried out to further investigate the e-p'-Vs relationship for Ottawa sand as well as for two tailing sand materials. The interest in tailings sands stems from the awareness that these cohesionless materials are used in the construction of large tailings dams which must be designed to resist both static and dynamic loading conditions. The tailings sands included an angular tailings sand from a mine in Alaska (Alaska sand) and a subrounded to angular tailings sand from the Syncrude oilsand extraction operation at Fort McMurray, Alberta, (Syncrude sand).

Comparison of all three sands tested will be presented and some generalizations about Vs measurements can be made. By combining the results of the in-situ testing and this laboratory testing a criterion based on shear wave velocity to delineate between soil which is susceptible to contraction (and possibly flow liquefaction) or dilation can be developed. From this developed relationship a suggested flow liquefaction evaluation is presented and worked examples of its use are given.

1.3 Organization of the Thesis

Chapter 2 of this thesis provides background information on the behaviour and modelling of cohesionless soils within the CSSM framework. The liquefaction phenomenon is discussed and its terminology presented. The background of shear wave velocity measurement is also discussed. This chapter also contains a section that develops the equations that define the large strain contractive/dilative boundary for a soil in terms of the parameters developed in this study.

Chapter 3 describes the laboratory triaxial testing program with Vs measurement undertaken in this research. It also describes all the cohesionless soils tested

Chapter 4 presents the test results for the Vs and ultimate steady state data for all three soils tested. The primary analysis of the data for the development of each soils specific e-p'-Vs relationship is presented. Scanning electron microscope analysis of the three sands is presented and discussed in this chapter.

Chapter 5 presents the analysis of the results and compares the different sands tested and makes some generalizations about the use of the Vs in evaluation of deposits of cohesionless soils. The analysis here uses the e-p'-Vs relationship and CSSM to develop a Vs against vertical effective stress relationship which gives the boundary for contractive/dilative behaviour for large strain loading. A suggested flow liquefaction evaluation procedure is presented and is compared to other existing flow liquefaction approaches.

Chapter 6 provides two worked examples of the suggested flow liquefaction procedure developed in the Chapter 5. A summary of all the work is also presented

Appendix A describes the triaxial testing in detail.

2.0 Background Information

2.1 Critical State Soil Mechanics (CSSM) Concepts

According to CSSM concepts a soil element exists in a state of void ratio and stresses such that it is either wet (loose) or dry (dense) of steady/critical state (SS/CS). A three dimensional space of void ratio (e), mean normal effective stress (p') and deviator stress (q) can be used to describe boundaries that separate the states at which a soil can or can not exist. These are state boundaries. It can also be used to describe a line called the ultimate steady state line (USSL) toward which, upon loading in shear, the soils conditions will ultimately move. A schematic plot of the general three dimensional space is shown in Figure 2.1.

For cohesionless soils the terms loose and dense are often used. A loose soil loaded in shear contracts to reach USS and a dense soil dilates to USS, both independent of the type of loading. This loading can be dynamic or static. In geotechnical design it is loose cohesionless soils that can produce large deformations and thus can be more critical for design. Dense cohesionless soils are typically not a design problem as they will not exhibit large deformations upon most loading conditions.

Thus the investigation of cohesionless soils is often directed toward quantifying how loose the soil deposit is in-situ. When a cohesionless soil is loose of USS and is sheared undrained it tends to contract and may strain soften, thus exhibiting a collapse behaviour. The soil can reach its peak strength but then strain soften rapidly to its steady state or residual strength. At this steady state there is a state of constant void ratio, effective mean normal stress and shear stress.

If a natural or man made slope of a loose strain softening cohesionless soil exists in a condition such that the in-situ static shear stresses are greater than the ultimate steady state strength, a catastrophic collapse and flow slide can occur if the strain softening response is triggered. The undrained loading condition to trigger the strain softening response can be either dynamic such as from earthquake loading or cyclic wave loading. Strain softening response can also be triggered by a static drained loading such as the slow rising of the water table (Sasitharan, 1994). An engineering evaluation into the

5

stability of such a slope would involve evaluating how much of the entire profile of soil is susceptible to collapse and hence flow liquefaction.

Much research into the behaviour of loose sands has taken place for both conditions of static and dynamic loading. Most current practice for the evaluation of the susceptibility of a soil to flow liquefaction is based on comparison of in-situ tests such as SPT or CPT.

With the SPT the evaluation is carried out by comparing the measured N at the site to a historical data base of information at sites that have or have not liquefied under past earthquake loading. In order to apply these data base values to all ground conditions, general correction factors have been developed. However it appears that for sloping ground these correction factors are too conservative (Robertson, 1993).

The CPT results can be compared in a similar manner as the SPT. However, some approaches exist that include CSSM concepts (Been and Jeffries, 1985). These methods test the soil in-situ and give an estimate of whether the soil is either loose of critical state and therefore contractive, or is dense of critical state and dilative. If a soil in-situ is loose of critical and contractive then the potential for flow liquefaction exists.

It has been shown by many researchers (Been et al., 1991; Roscoe et al., 1958; Castro, 1969) that the initial state, in terms of void ratio and effective stress, of a soil can be used to determine the steady/critical state and hence the large strain behaviour.

Recently the use of the Vs as a tool for the prediction of soil state has gained interest by researchers. Vs measurements in soil has the advantage over other in-situ tests in that it can be measured both in-situ and in a number of geotechnical testing devices in the laboratory. Another advantage of Vs is that the Vs evaluation can proceed independent of the SPT evaluation and that the concepts of CSSM can be embedded in this Vs approach.

CSSM will be used as a framework for describing the test results and modeling of the cohesionless soils investigated in this research. Its concepts will also be used along with the developed e-p'-Vs relationship for cohesionless soils to produce a flow

liquefaction evaluation procedure. For this reason a brief discussion of CSSM development, how it is applied, and its current use in engineering practice follows.

2.1.1 History and Development of CSSM

The concept of CSSM was presented by Roscoe *et al.* (1958) to describe the behaviour of clays. The authors described the behaviour of remoulded saturated clays in a three dimensional space of deviator stress (q), mean effective stress (p'), and void ratio (e). The authors showed that a line existed in this space to which all samples ultimately reached with a state of constant shear stress, effective stress, volume and with constant deformation. They termed this line the critical void ratio line (CVRL). Tests were done in a drained and undrained manner and results described in terms of the CVRL in the plots of e-q-p'.

Roscoe *et al.* (1958) summaries that remoulded saturated clay in triaxial compression has a characteristic yield surface which contains the CVRL within the e-q-p' space to which the loading paths converge at high strains. The authors also looked at the behaviour of cohesionless granular media and silt material and suggested that they should also follow the same framework. Roscoe *et al.* (1958) also suggested that the initial state of the soil defines the ultimate state.

It was not until the work of Castro (1969) that this framework was applied to cohesionless soils. He carried out extensive testing on loose cohesionless soil in monotonic and cyclic undrained stress controlled loading. Castro (1969) showed that loose sands can strain soften and reach a steady state and that the void ratio was the most important factor controlling the steady state.

Been and Jeffries (1985) introduced the state parameter to describe the large strain behaviour of a sand based on the combined influence of the initial void ratio, effective confining stress and their relation to the steady state void ratio at the same stress. This showed that the initial state of a sand controlled its large strain behaviour. State parameter is defined as the difference in void ratio between the in-situ void ratio and the void ratio at steady state at the same mean normal effective stress level. Been and Jefries (1985) show that the state parameter can be related to a number of soil properties

including normalized peak undrained strength, pore pressure parameter at failure, angle of phase transformation (PT), peak angle of shearing resistance, and dilation rate

A sketch of this definition of the state parameter (Ψ) is shown in Figure 2.2. This figure also shows the USSL and the zone of dilatant response which is below the USSL and the zone of contractant response above the USSL. A positive Ψ indicates contraction to USS and a negative Ψ indicates dilation to USS.

Further development in CSSM of sands was the concept of a collapse surface to describe the behaviour of very loose sands by Sladen et al. (1985a and b). They suggest that the concept of critical state is the same as steady state for cohesionless material based on a large data base of tests on sands from offshore island construction. From the data base Sladen et al. (1985a) concluded that strain controlled and stress controlled tests give the same result.

Sladen et al. (1985a and b) showed that in p'-q-e space a surface exists that would trigger collapse and strain softening in undrained shear. Further work on the collapse surface by Alarcon-Guzman et al. (1988) described the collapse of sands in the framework of state conditions marking initiation of the strain softening behaviour for both monotonic and cyclic loading conditions. Both authors use the peak p' and post peak portion of the undrained stress path to define the collapse surface.

Been and Jeffries (1991) showed that it was the soils initial state that defined its ultimate steady state regardless of the stress path taken in loading. That is, steady state is independent of the stress path and is also the critical state. The authors also gave evidence that the steady state of a sand was unique. Ishihara et al. (1991) illustrated the collapse behaviour of loose sands with a number of different laboratory tests and a variety of case studies of flow liquefaction in the field in sands using CSSM framework

All previous investigations in collapse mechanics were postulated based on undrained conditions. Flow slides in coaking coal, a material similar to a sand, were investigated by Eckersly (1990) who showed that a collapse of a loose sand could be triggered by a static drained loading. This showed that collapse was not just related to dynamic loading or undrained conditions.

This was investigated further by Sasitharan (1994) who defined the collapse surface for a loose sand and set up the equations that define the collapse surface in p'-q-e space. He found that collapse could take place whether loading was drained or undrained. Thus Sasitharan (1994) defined a state boundary for sands.

CSSM is described in detail in books by Scofield and Wroth (1969) and by Atkinson and Bransby (1977).

2.1.2 Steady/Critical State Concept

Steady state was defined by Poulos (1981) as a state of constant volume, shear stress, mean normal stress and velocity. His tests were stress controlled and steady state probably was at a constant velocity, although no measurements of this velocity were made. Poulos (1981) states that steady state is only reached when the particle orientation is at the steady state condition.

Critical state as defined by Roscoe et al. (1958) is a state of continued deformation at constant shear stress, mean normal effective stress, volume and deformation rate. Roscoe et al. (1958) does not give an indication of the value of this deformation rate.

2.1.3 Ultimate Steady State

The ultimate steady state (USS) is the steady state reached by straining a sample to large deformations of about 20% axial strain. It is also a state of constant q, p', e, and deformation rate and thus a steady state. This should be synonymous with steady state/critical state and will therefore be used throughout this paper as USS. USS is a term that will be used in this research to describe steady state and critical state at large strains.

Ishihara (1993) refers to the USS in his Rankine lecture as the state at large strain. He also refers to a quasi steady state (QSS) which by his definition was seen in some of the testing in this research, but was not as clearly defined as USS. The term QSS is deceiving because it is not really a steady state. The terminology of the phase transformation (Vaid and Chern, 1985) will be used here for the soils that exhibit this type of behaviour.

2.1.4 USS Parameters

Following the framework set up by Roscoe *et al.* (1958) the behaviour of a cohessionless soils will be described mathematically by CSSM. The same three dimensional space of void ratio (e), the mean normal effective stress (p'), and the deviator stress (q) will be used. With the following definitions for a triaxial test,

$$p' = 1/3 \times \{\sigma'1 + (2 \times \sigma'3)\} \tag{1}$$

$$q = (\sigma'1 - \sigma'3) \tag{2}$$

where; $\sigma'1$ = effective stress in the major principal direction

$\sigma'3$ = effective stress in the minor principal direction.

p' = the first invariant of the stress tensor

q = the second invariant of the stress deviator tensor

A schematic plot of this three dimensional space with the USSL is shown in Figure 2.1. In order to see this information more clearly it is common to show the data on two planes. These two planes are shown schematically in Figure 2.3. Figure 2.3a shows the e against log p' plane. This is used to show the consolidation data as well as the USSL. Figure 2.3b shows the normalized stress paths using a normalization suggested by Sladen and Oswell (1989). This normalization removes the effect of different void ratio so tests at different void ratios can be compared. The normalized stress path is presented as a (p'/p'uss) against (q/p'uss) which maps the development of p' and q in shear loading. The USSL is seen as a point in this plane and the collapse surface is seen as a line. Also shown in Figure 2.3b is the constant volume friction angle (ϕcv) line. This is shown as a line from the origin through the USS point with a slope M which is related to the mobilized friction angle (ϕ) as;

$$M = \frac{6 \times \sin(\phi')}{(3 - \sin(\phi'))} \tag{3}$$

The CSSM parameters for describing a soil are obtained from these two diagrams The values are as follows;

Γ = the intercept of the USSL at p' = 1 kPa in e against log p'

λ = the slope of the USSL in e against log p'

M = quss/p'uss

s = the slope of the collapse surface in the stress path plot through the USS point (Sasitharan 1994).

The phase transformation (PT) can be defined as an angle in the normalized stress path plots. It is the angle defined by the ratio of q and p' ($=M_{PT}$) from the origin to the elbow in the stress path and can be obtained by inserting M_{PT} in equation (3) and solving for ϕcv. This is not shown on the schematic of Figure 2.3.

2.1.5 Application of CSSM

With conflicting literature on CSSM over the years there is a need to have a more unified approach for applying CSSM concepts for cohessionless soils. Geotechnical engineering should embody these concepts in many of its evaluations and correlation procedures.

A summary of the present day thinking of CSSM concepts is added here in terms of the liquefaction phenomena.

2.2 Liquefaction Phenomena

A principal goal of this research was to develop an e-p'-Vs relationship to define, within the concepts of CSSM, a contractive/dilative boundary within the Vs and vertical effective stress (σ'_v) space. This marks the boundary between a state at which a soil could be susceptible to contraction or dilation in shear loading. If the soil is able to contract and strain soften then the possibility for flow liquefaction exists. If the material is dilatant then it is not susceptible to flow liquefaction.

Liquefaction has been widely used in geotechnical engineering for the description of a number of different events. Hence, a discussion is given here to define what is meant by liquefaction.

Liquefaction as defined by Cassagrande (1976) describes the flow of loose saturated sands. Castro (1975) discussed how a loose soil can lose a large part of its peak

11

shear resistance during undrained monotonic, cyclic or shock loading and flow like a liquid until the stresses acting on the mass are as low as the reduced shear resistance

The analysis of a soil deposit for liquefaction presently relies heavily upon the SPT N value and an empirical historical database of SPT N. The database is largely for level ground conditions and correction factors have been developed to apply this database of information to sloping ground. However, many practicing engineers are finding cases where this approach is too conservative (Byrne *et al.*, 1993). Thus one of the objectives of this research is to provide a framework to use Vs to detect soil that is contractive or dilative and hence susceptible to flow liquefaction.

2.2.1 Liquefaction Terminology

According to definitions set out by Robertson (1994) the following will be used for description of cohesionless soil behaviour in various loading conditions. Robertson (1994) proposed a flow chart for evaluating liquefaction of a cohesionless deposit of soil. This chart is a good summary of the design process that would be used in a liquefaction evaluation and is shown in Figure 2.4.

Generally it divides the liquefaction problem into two cases of either a) flow liquefaction or b) cyclic liquefaction/mobility. The first, flow liquefaction, requires a strain softening response during undrained shear. The trigger can be either static or dynamic loading. Flow liquefaction requires that the in-situ shear stress be greater than the ultimate steady state resistance. If there is a sufficient amount of this type of material in a deposit then large uncontrolled deformations can be expected. If this type of material is limited in the deposit or the geometry is such that it confines the deposit then smaller deformations can be expected. In both cases deformations can continue to occur after the triggering event.

Cyclic liquefaction/mobility are both triggered by undrained cyclic loading. Cyclic liquefaction occurs if the in-situ shear stresses are small and if shear stress reversal occurs during cyclic loading leading to a condition of zero effective stress which can resulting in large deformations. This condition of zero effective stress generally stops when cyclic loading stops and thus deformations should stop. Cyclic mobility occurs

12

when the in-situ shear stresses are large and shear stress reversal can not take place. The deformations expected are not large and they occur only during the cyclic loading.

In terms of CSSM the soils initial conditions can lead to either strain softening response (ss), limited strain softening response (LSS), or strain hardening response (SH) to undrained shear. Figure 2.5 shows the locations of these points in an e against log p' plot. The consequences of liquefaction depend upon the initial soil state at the time of the event. If a cohesionless sand is loose, such as ss in Figure 2.5, and is sheared undrained it can achieve a peak strength at a very small strain, in the order of 0.5% followed by a strain softening behaviour. In stress path space the stress path appears to rise up until it hits what is termed a collapse surface and then falls rapidly to ultimate steady state.

If the in-situ static shear stress is greater than the ultimate state shear resistance, then flow liquefaction is possible with large flow like deformations expected. However, if the static shear stress is less than the steady state shear resistance then no large flow liquefaction is expected and deformations can be small.

Some loose sands when sheared undrained can exhibit strain hardening to attain steady state, however, a very low confining stress is required. A medium dense sand such as at the LSS point in Figure 2.5 may strain soften a small amount but will ultimately strain harden to reach USS. An elbow is noted in the stress path at the PT. For the medium dense sand the steady state shear strength will be higher than the loose sand. For a dense sand such as SH in the Figure 2.5 the expected behaviour is to strain harden when sheared undrained. The ultimate steady state shear strength will be very high. However, if the confining stresses are extremely high, greater than 1000 kPa the sample could exhibit a contractive behaviour to steady state (Sasitharan 1994).

It is important when evaluating the in-situ state of a soil to decide whether the soil will either contract to steady state and perhaps strain soften, or if it will dilate and strain harden.

2.3 Shear Wave Velocity Measurement

Interest in the Vs of soil has been increasing as an investigation tool of soil behaviour over the past number of years. Initially Vs was used by geotechnical engineers primarily to analyze soil foundations for dynamic loading problems. This work will show how Vs can be used as an indicator of in-situ state and how it can be used to predict the large strain response of the soil.

In the field, Vs can be measured by intrusive methods such as seismic cone penetration test (SCPT) (Robertson *et al.*, 1986), or by downhole or crosshole seismic techniques. Non intrusive methods include the spectral analysis of surface waves (SASW) method. The SASW can give an almost continuous profile of Vs with depth where the intrusive methods give Vs at discrete depths usually some 0.5 to 1.0 meters apart.

In all cases a shear wave is generated by a source at the surface or down a borehole and the travel time of the wave is measured as it travels to the receivers at a known distance from the source. The result is the distance and time of shear wave, producing the Vs.

Vs is a body wave which has the particles in motion perpendicular to the direction of propagation. Thus Vs is controlled by the stress conditions in the two directions. Elastic theory relates Vs with the small strain shear modulus (Go) and soil mass density (ρ) as;

$$Go = \rho \cdot Vs^2 \tag{4}$$

Thus with the mass density known, Vs and Go are synonymous. Throughout this research the Vs is the preferred parameter as it is the parameter that can be measured directly in the field.

Elastic theory assumes that elastic waves propagate in a material which is assumed to be linear elastic, homogeneous, and isotropic. If the shear strain to measure shear modulus (G) is very small, in the order of $10^{-4}\%$, then this is termed Go. Most field and laboratory techniques measure Vs at very small strains.

Work by Hardin and Black (1968) suggests that the small strain shear modulus (and hence Vs) is related to soil properties as follows;

$$G_o = F(p', e, H, S, \tau o, C, A, f, t, Ss, T) \tag{5}$$

where
p' = mean principal effective stress
e = void ratio
H = ambient stress history
S = degree of saturation
τo = octahedral shear stress
C = grain characteristics, grain shape, grain size, mineralogy, grading
A = strain amplitude
f = frequency of vibration
t = secondary effects that are functions of time and secondary loading
Ss = soil structure
T = temperature

Hardin and Black (1968) and Knox *et al.* (1982) have shown that the two most important parameters controlling Vs are the void ratio and the effective stress condition. The soil fabric is of secondary importance and the other parameters are of generally much less importance to the Vs.

Hardin and Richart (1963) also showed that the Go (or Vs) is primarily a function of both the void ratio and mean normal effective stress (p'). They suggested a relationship between Vs, e and p' in the form of;

$$Vs = (m_1 - m_2 e) * (p')^{0.25} \tag{6}$$

where m_1 and m_2 are constants determined for each soil and reflect the influence of the other factors in equation (5).

15

2.3.1 History and Development of Shear Wave Velocity Measurement in the Laboratory

Go can be measured in the laboratory with the resonant column device (RC). The RC is based on a theoretical solution that relates dynamic modulus of a column to its resonant frequency. The RC can apply a confining pressure and in recent years can also handle saturated soils.

A number of studies with the RC device reported both the measured small strain elastic modulus (Go) and soil damping properties from the decay of the vibration. Work has been carried out by Hall and Richart (1963), Hardin and Richart (1963), Hardin and Drnevich (1972a and b) and many others on various soils in the RC in order to determine dynamic properties.

Some advantages of the RC include that the shear strain can be measured and that the damping properties of the soil can be determined. Some disadvantages include that the device can not load the sample to large strain and that the equipment is complicated.

More recently Vs can be measured in the laboratory with the use of ultrasonics. Ultrasonic methods include piezoceramic crystals and bender elements. Work to measure Vs with crystals has been carried out on material such as spray ice (Instanes, 1993). Work on Vs measurement with bender elements is described in detail in Section 2.3.1.2.

It was Shirley (1978) who introduced the use of the bender element for measuring Vs in soils in geotechnical laboratory testing devices. A brief description of bender elements and the history of their use follows.

2.3.1.1 The Bender Elements

Bender elements are made up of two long, thin sheets of piezoceramic material rigidly bonded along their lengths to become an electro-mechanical transducer. When a 180° out of phase voltage is applied to the element one of the sheets will expand and the other will contract. This results in a back and forth bending motion which if positioned correctly will create a transverse (shear) wave.

Bender elements have the capability of acting as both a source which converts electrical signals to mechanical signals and a receiver which converts a mechanical signal to electrical signal. Thus bender elements can be used in soil samples to transmit an electrical wave into a mechanical (shear) wave at one end and to be used as a receiver of the mechanical (shear) wave which can be converted into an electrical wave.

If the bender is in contact with soil it will create a very small strain shear wave. This wave will travel the length of the soil and create motion in the receiving bender element. With the use of an oscilloscope, a wave generator and an amplifier/converter, the input electrical wave can be compared to the received amplified electrical wave and using the first pulse arrival method, the shear wave travel time can be obtained from the oscilloscope. Knowing the distance separation of the bender elements along with the travel time of the shear wave, the shear wave velocity may be calculated.

The bender elements used in this research were supplied by Piezo Systems Inc. of Cambridge, Mass.

2.3.1.2 Previous Shear Wave Velocity Testing Using Bender Element Technology

Shirley (1978) and Shirley and Hampton (1978) introduced the use of a bender element device to measure the Vs in laboratory prepared soils and in unconsolidated marine sediments. Horn (1980) updates the use of bender elements to measure the Vs from the use of resonant column and feels that there is potential to develop the relations between geophysical properties and geotechnical properties. Horn (1980) finds that the received shear waves have a unique reversible form if the source is reversed. This can be used to distinguish them from compression waves which have the same form for a reversed source.

Strachan (1981) looked at the correlation of Vs and compression wave velocity (Vp) to the dynamic properties of sands in a marine environment. Schultheis (1981) used bender elements to measure shear wave velocity in the laboratory in marine sediments. He installed benders in the oedometer and noted a changing Vs with increasing load. This was mainly because both the e and p' were changing although the author did not quantify the results in that manner.

17

Dyvik and Madshus (1985) and Dyvik and Olsen (1991) measured Vs using bender elements in a number of geotechnical testing devices including the triaxial cell, oedometer, and the direct simple shear. They also measured Vs directly in the resonant column device and compared Go from bender elements to Go obtained from the resonant column for a cohesive soil. They found the two shear moduli agreed very well with each other for a range of Go from 5 to 140 MPa. They also detail the electrical wiring of the bender elements in order to optimize them for generating and receiving of waves

De Alba *et al.* (1984) used cyclic triaxial tests to relate shear wave velocity to liquefaction potential of saturated sands. The bender elements were built into the ends of the triaxial test device. The authors suggest that Vs offered a method to overcome preparation effects in reconstituted samples. If the Vs of the laboratory sample is matched to the in-situ Vs then the test should give the in-situ liquefaction resistance. The authors suggest this direct testing of soil helps to overcome the empiricism that surrounds the methods of SPT for the purpose of liquefaction resistance.

Thomann *et al.* (1990) used bender elements to measure Vs in sand under varying coefficient of earth pressure at rest (Ko) conditions (no lateral strain). He also tested Ottawa sand and a silt material in the resonant column with bender elements installed to show that the Go from benders agrees well with Go from resonant column for a range of Vs from 170 - 340 m/s.

2.3.2 Previous Studies on use of Vs

Work by Hardin and Richart (1963) showed that there was a relationship between e-p'-Vs for isotropically consolidated samples. Later Roesler (1979) investigated the relationship for anisotropic consolidation. Roesler (1979) found that plane shear waves travelling through a soil caused shear strains only in the direction of wave propagation and polarization. Thus the stresses that affected the Vs were only the stresses in the direction of propagation and polarization and the third perpendicular stress had no effect

Stokoe and Naxarian (1985) suggest a Vs of 140 m/s as a boundary of liquefaction based on six field site that did and did not liquefy during both the 1979 Imperial Valley and 1981 Westmoral earthquakes in California

Work by Tokimatsu and Hosaka (1986) showed that Vs could be used to quantify sample disturbance The authors compared tests on laboratory samples obtained from both tube samples and from in-situ freezing The results showed a different Vs in the two samples obtained by the different methods.

Further work by Tokimatsu *et al.* (1986) related Go to liquefaction resistance The authors describe a technique of reconstituting the sample in the laboratory and consolidating until the Go is matched to the field measured value This would reproduce the field state of the soil and its liquefaction resistance could be determined

Stokoe *et al.* (1988a and b) investigated field measured Vs to determine the boundary of the potential for liquefaction They used the computer program SHAKE and a field case example to develop a correlation between the Vs and the maximum ground acceleration (a_{max}) based on various stiff soil sites and the number of cycles of strong motion.

Tokimatsu and Uchid (1990) related the cyclic resistance of a soil to its shear wave velocity They defined liquefaction as the stress ratio to cause double amplitude of 5% in 15 cycles This is a very specific liquefaction definition and does not include the CSSM concepts

Robertson *et al.* (1992a) normalized the shear wave velocity with respect to vertical effective stress (σ'_v) with a stress exponent of 0.25 to get the normalized shear wave velocity (Vs1) They developed a criteria which separates the contractive from dilative response They suggested that a Vs1 value of greater than 160 m/s would not exhibit flow liquefaction potential

Sasitharan (1994) used bender elements to measure shear wave velocities to determine sample disturbance upon freezing and thawing in laboratory prepared specimens The results showed that if no disturbance took place upon freezing or thawing then the Vs was unchanged Sasitharan (1994) also developed a relationship for clean Ottawa sand using shear wave velocity and vertical effective stress to define the boundary between conditions of flow and no flow.

19

2.3.3 Vs and the CSSM Concepts

The work of Sasitharan (1994) combines the concepts of Vs and CSSM. This is the basis of this research and is discussed here.

It has been shown that Vs is mainly a function of both void ratio and mean normal effective consolidation stress (p'c) for isotropic consolidation state. CSSM provides a relationship between the e-p'-q for ultimate steady state of the soil due to any loading condition. The concept of the state parameter can be used to combine Vs and CSSM. If Vs is measured in the field and an assumption of Ko is made to obtain the in-situ p' with depth, then an initial state of the soil can be estimated with the Vs-e-p' relation. With the CSSM USS parameters this state can be compared to the USSL. Thus it can be seen if the soil is contractive or dilative under large strain loading.

2.3.3.1 The e-p'-Vs Relationship

The development of the e-p'-Vs relationship is derived from the laboratory tests carried out in this research. The basis of the relationship follows that of Hardin and Richart (1963) as well as Roesler (1979). Roesler (1979) gave the equation,

$$Vs \, \propto \, \sigma'_a{}^{0.149} * \sigma'_b{}^{0.107} * \sigma'_c{}^{0.0} \tag{7}$$

where, σ'_a = effective stress in direction of the shear wave propagation

σ'_b = effective stress in direction of the particle movement

σ'_c = effective stress in the direction perpendicular to a and b

Note that the sum of the powers adds up to 0.256 which is very close to the 0.25 many other researchers have shown for the mean effective stress and that the third perpendicular stress has no effect on Vs

Yu and Richart (1984) studied stress ratio effects in Vs and they found that if Ko was less than 2, equation (7) for shear wave velocity was still valid

During the tests conducted in this research program Vs was measured during isotropic consolidation such that the following condition is valid.

$$\sigma'_a = \sigma'_b = \sigma'_c = p'c \tag{8}$$

This allowed the Vs normalization to be carried out with p'c. Vs was also measured at the ultimate steady state. This required the individual stress normalization to be applied to compare these results with those at consolidation.

The tests in this research measured e, p', and Vs as accurately as possible by laboratory standards. The three variables can compared by normalizing Vs with the p' and comparing the normalized shear wave velocity (Vs1) with the e. The normalization takes the form of the following;

$$Vs1 = Vs \cdot (Pa/p'c)^{(n)} \tag{9}$$

where, Vs1 = normalized shear wave velocity, m/s

Vs = measured Vs at known p' and e, m/s

Pa = reference pressure, (usually 100 kPa)

p'c = mean effective consolidation stress, kPa

n = stress exponent

For this study stress will be given in units of kN/m^2, hence $1000\ Pa = 1\ kN/m^2$.

The data gathered in tests of Vs1 and e could be statistically averaged to determine the Vs1 - e relation in the form,

$$Vs1 = \{A-(B \cdot e)\} \tag{10}$$

where, Vs1 = normalized Vs, m/s

A = intercept of the Vs1 - e relationship at e = 0, m/s

B = slope of the Vs1 - e relationship, m/s

e = void ratio

Combining equations (9) and (10) the following e-p'-Vs relation could be determined from the laboratory testing data;

$$Vs = \{A-(B \cdot e)\} \cdot (p'c/100)^{(n)} \tag{11}$$

where: Vs = shear wave velocity, m/s

A, B = constants determined from laboratory tests, m/s

p'c = mean normal effective consolidation stress, kPa

n = stress exponent

It is this relation that can be used to estimate the field void ratio from the field Vs and field effective stress conditions. To determine the field effective stress conditions the soil bulk density, ground water table location and Ko must be known.

With this relationship and USS parameters the location of the state within the soil deposit relative to the USSL can be determined. Hence, the determination of either contractive or dilative behaviour upon loading is made.

Determination of the A and B constants in the p'-e-Vs relationship was from linear regression of the consolidation data for each sand tested. The stress exponent (n) of the normalization was varied for each material.

2.3.3.2 Vs for the Evaluation of Flow Liquefaction.

Robertson *et al.* (1992b) suggest that an initial step in a liquefaction evaluation study should be to determine if the large strain response of the soil is contractive or dilative. If it is contractive then the main issue is to design against the potential for flow liquefaction. If it is shown to be dilative no flow deformations are expected, however, it may need to be investigated for cyclic liquefaction/mobility.

A procedure for determining the soil contractive/dilative boundary in terms of the e-p'-Vs relationship and the USS parameters will be developed here. This boundary will be presented for the Vs value that defines the boundary which varies with a given $\sigma'v$.

Since field conditions are not always isotropic, an individual stress exponent form of equation (11) above will be used. The individual stress exponents are assumed to be half of the total stress exponent. This produces the equation;

$$Vs = \{A-(B \cdot e)\} \times (\sigma'a/100)^{n/2} \times (\sigma'p/100)^{n/2} \qquad (12)$$

where; $\sigma'a = \sigma'v$ = axial or vertical effective stress in kPa

$\sigma'p = \sigma'h$ = perpendicular to axial or horizontal effective stress in kPa

This can be reduced with the following stress ratio equation

$$Ko = \sigma'h/\sigma'v \tag{13}$$

which gives the equation;

$$Vs = (A-B \cdot e) \times (\sigma'v/100)^n \times (Ko)^{n/2} \tag{14}$$

If the state parameter concepts are considered;

$$\Psi = e - ess \tag{15}$$

is combined with the CSSM definitions of ess;

$$ess = \Gamma - \lambda \log(p'uss) \tag{16}$$

they produce the combined equation;

$$\Psi = e - \{\Gamma - \lambda \log(p'uss)\} \tag{17}$$

Where (14) can be rearranged to get e = function of (Vs and σ_v') and gives;

$$e = \frac{A - Vs \times \left(\frac{100}{\sigma'v}\right)^n \times \left(\frac{1}{Ko}\right)^{n/2}}{B} \tag{18}$$

If equation (18) is combined with the state parameter equation (17) then;

$$\Psi = \left[\frac{A - Vs \times \left(\frac{100}{\sigma'v}\right)^n \times \left(\frac{1}{Ko}\right)^{n/2}}{B}\right] - \{\Gamma - \lambda \times \log(p'uss)\} \tag{19}$$

23

The p'uss in the equation can be replaced with $\sigma'v$ and Ko from;

$$p'uss = \sigma'v \times (1 + 2 \times Ko)/3 \qquad (20)$$

In the framework of CSSM if $\Psi = 0$ then the soil state is at the contractive/dilative boundary. Applying this to equation (19) with equation (20) and rearranging to present the result in terms of Vs gives the following;

$$(Vs)_{\Psi=0} = [A - B \times (\Gamma - \lambda \times \log\{\sigma'v \times (1 + 2 \times Ko)/3\})] \times (\frac{\sigma'v}{100})^{n} \times (Ko)^{n/2} \qquad (21)$$

Thus $(Vs)_{\Psi=0}$ is shown to be defined by the 4 soil constants, A, B, Γ, and λ as well as by the in-situ Ko. This $(Vs)_{\Psi=0}$ is a function of the vertical effective stress

Equation (21) defines the Vs value for $\Psi=0$ for a given $\sigma'v$ and can be plotted in a Vs against $\sigma'v$ plot with the (Vs) boundary shown to mark the boundary between contractive and dilative behaviour.

Thus by measuring the in-situ Vs, combined with the knowledge of the in-situ vertical effective stress and with the estimation of the consolidation state (Ko), the in-situ state of the soil can be estimated from the e-p'-Vs relationship. To develop this relationship requires that a number of laboratory tests on reconstituted samples of the appropriate sand be undertaken to determine the shear wave velocity constants A and B The samples can then be loaded in shear to determine their USS parameters

From the above it can be see that the shear wave velocity can be used to screen a soil profile for contractive and dilative response at large strains and thus the soils potential for flow liquefaction.

24
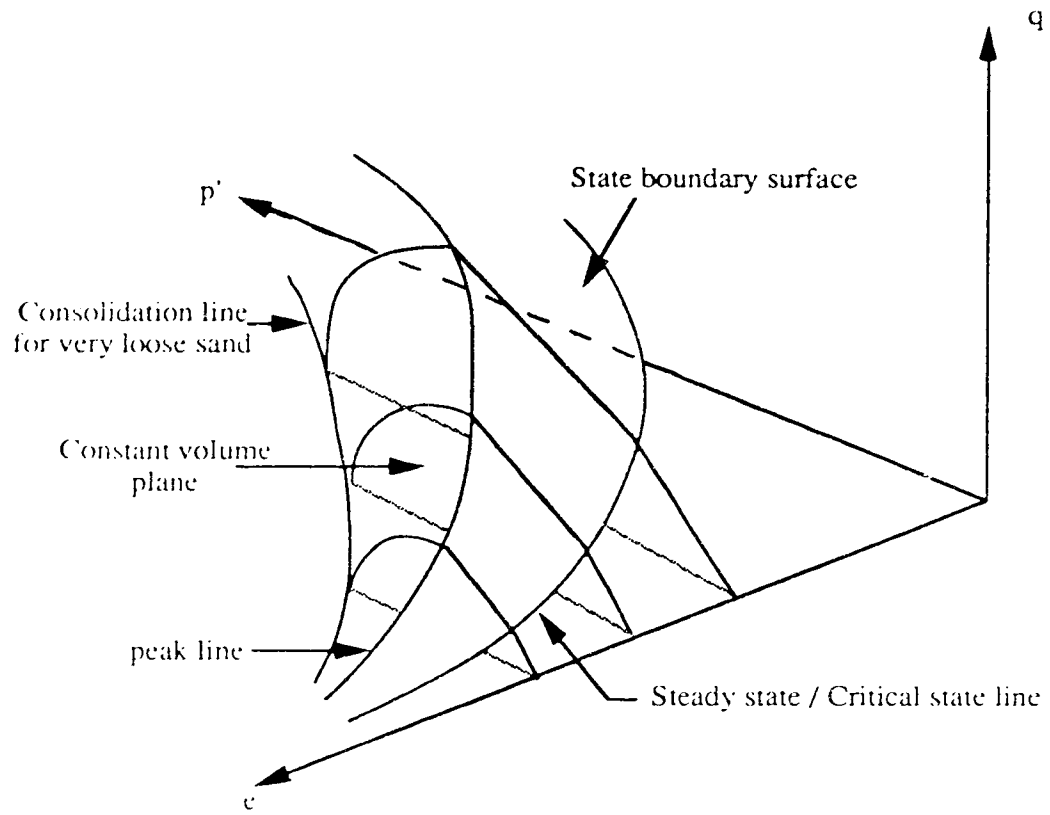
Figure 2.1 Schematic of the three dimensional CSSM framework for soil state and steady state representation, after Sasitharan (1994).

25

1

Contractive

Γ USSL

(e)

$\Psi = e - e_{ss}$

e

ess

Dilative

0.4

(p')

1   10   100   1000

p', (kPa)
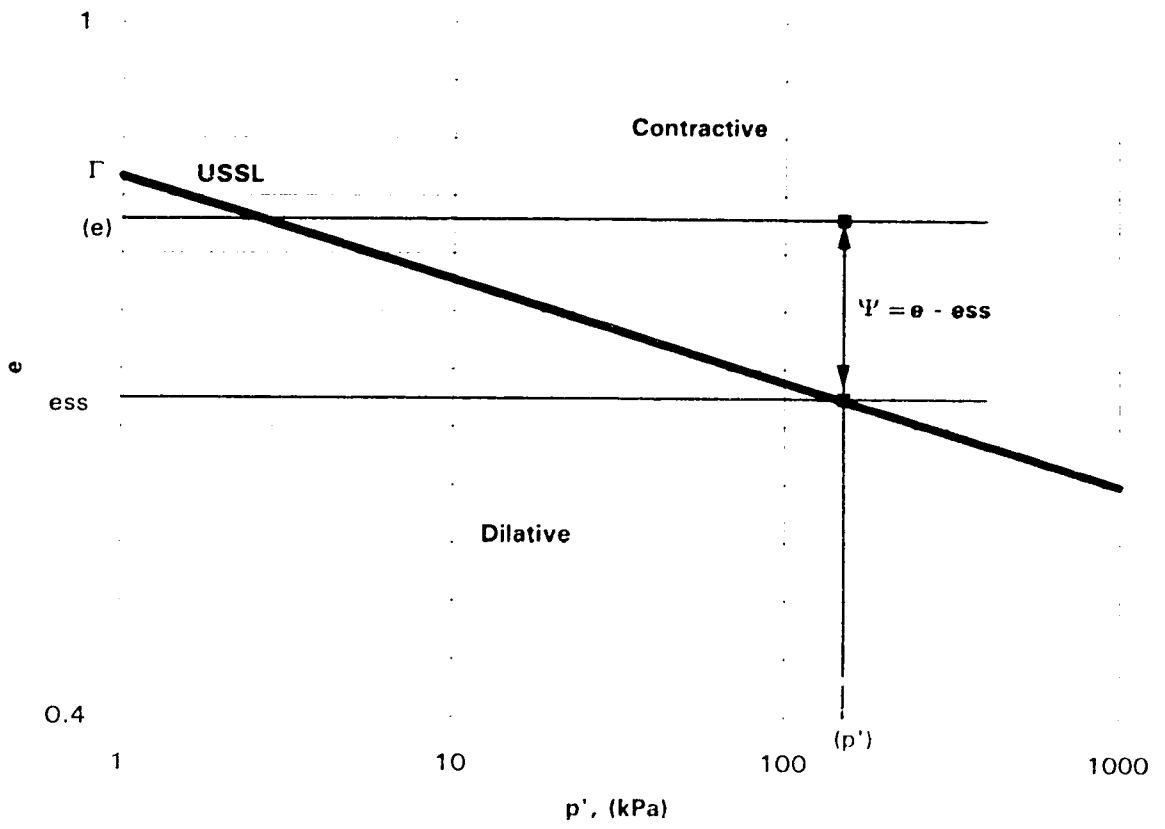
Figure 2.2 The state parameter.

a).

Chart axes: e,uss / e (vertical, 0.5 to 1), p', (kPa) horizontal (1, 10, 100, 1000)

Labels: Γ, USSL, Contractive, λ, 1 log cycle, Dilative, p'uss

b).

q/p' uss, (kPa) vertical axis (0 to 5)

p'/p'uss, (kPa) horizontal axis (0 to 10)

Labels: Collapse Line, USS Point, M, s, undrained stress path, drained stress path, M
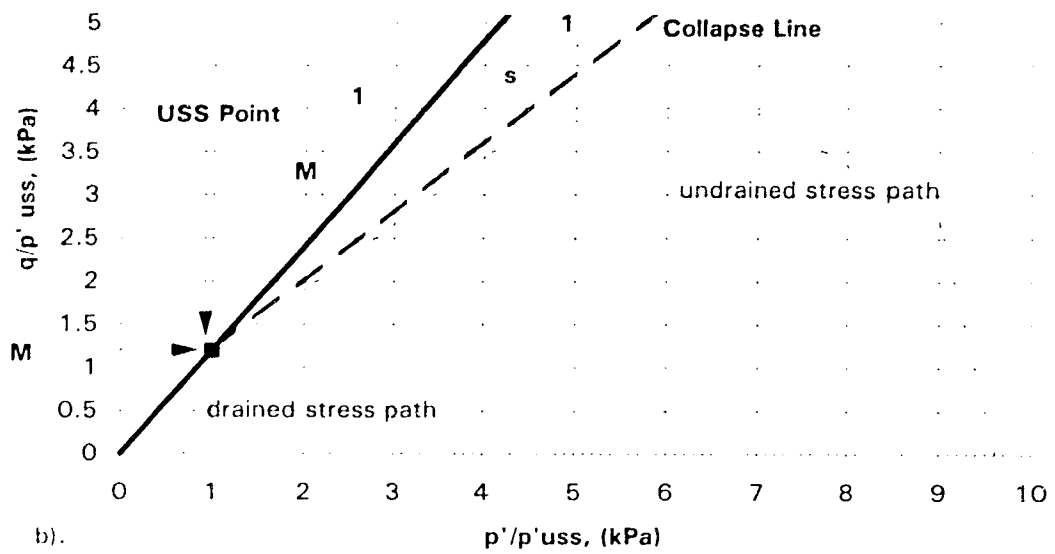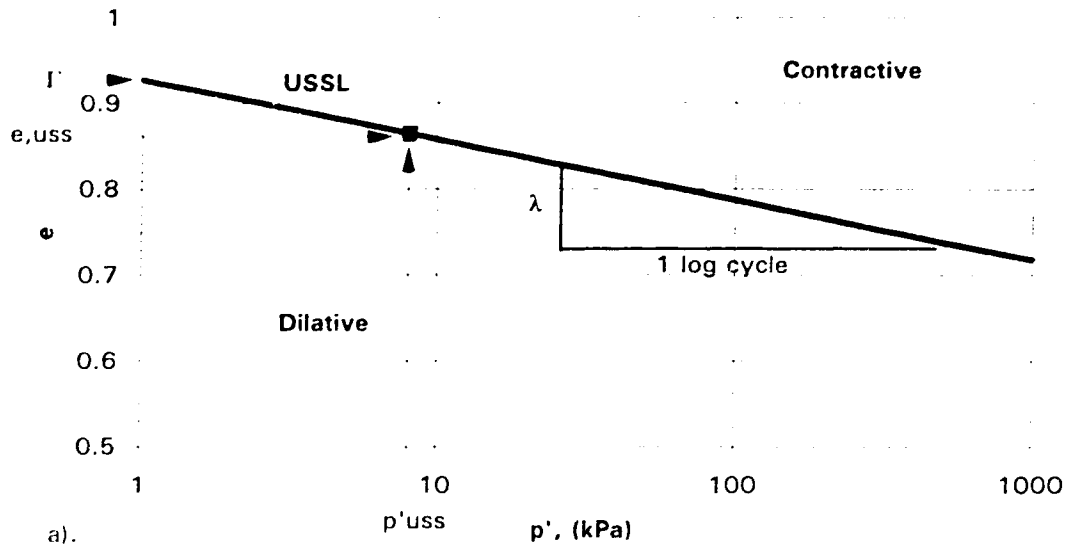
Figure 2.3 Definitions of the USS parameters in a). e against log p' space and b). in normalized stress path space.

27

FLOW CHART FOR LIQUEFACTION
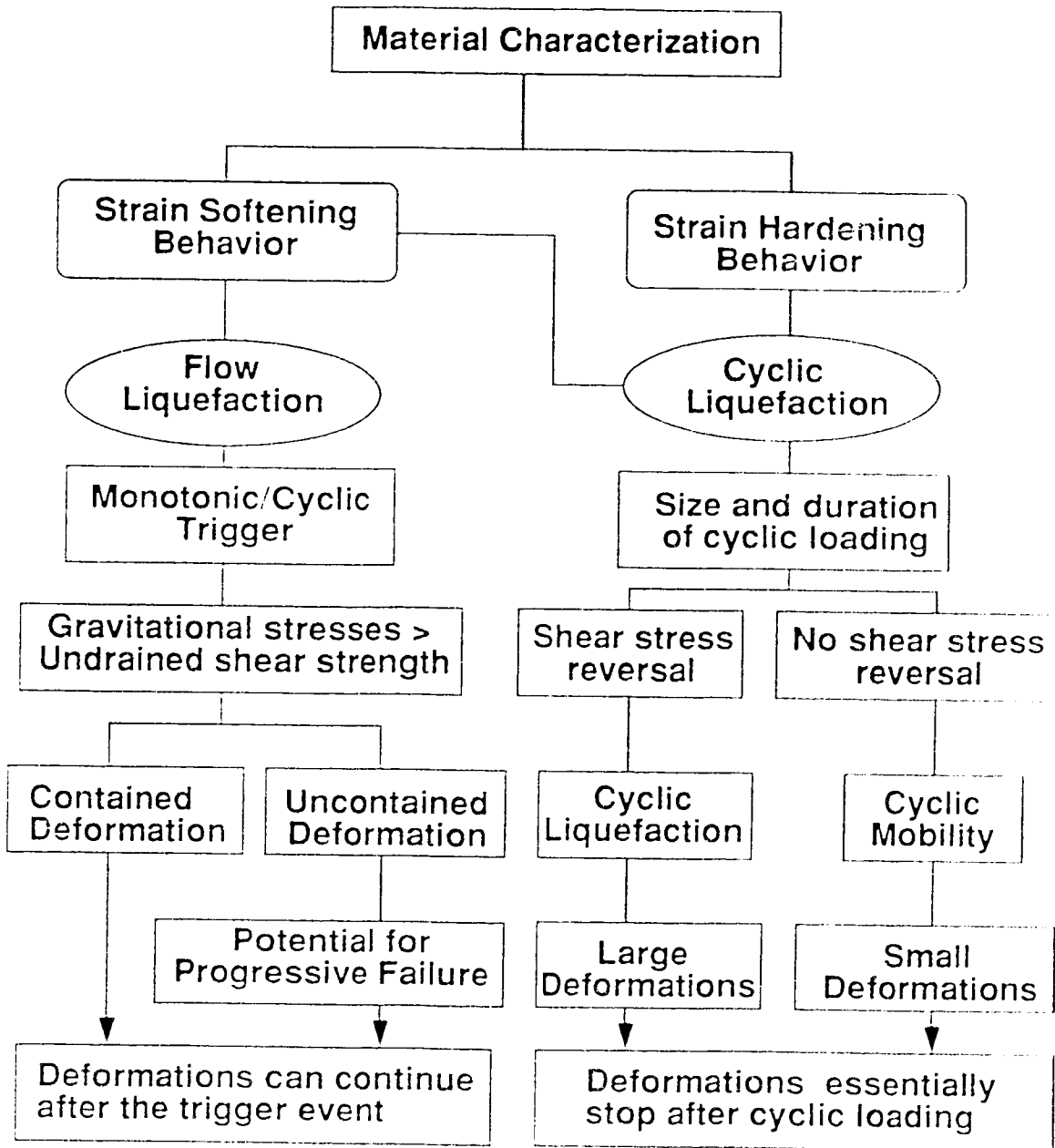
Figure 2-4 Flow chart for evaluation of liquefaction, after Robertson (1994)

28

Void ratio
e

o SS

o LSS

SSL/CSL

SH o

Mean effective stress, p'
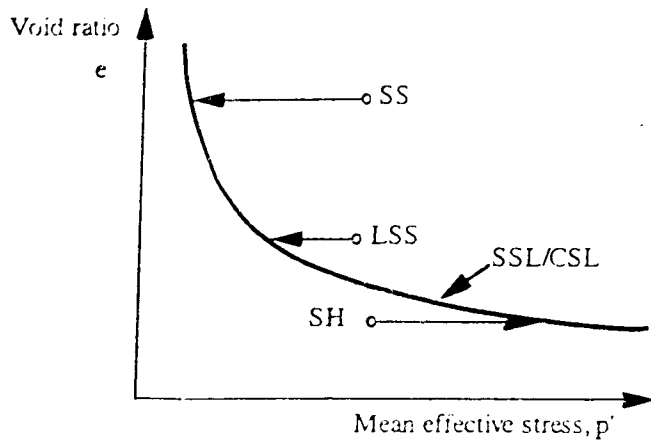
Notation:

SS: Strain softening response
SH: Strain hardening response
LSS: Limited strain softening response
q_{ST} : Static gravitational shear stress
Su: Ultimate undrained steady state
shear strength
SS/CS: Steady or Critical state

Shear stress
q

SS/CS

Collapse surface

SS

q_{ST}

P'

q

Strain softening (SS)

Su

γ, shear strain

q

SS/CS

LSS

q_{ST}

P'

q

Limited strain softening (LSS)

γ

q

Peak strength envelope

SS/CS

Phase transformation

SH

q_{ST}

P'

q

Strain hardening (SH)

γ
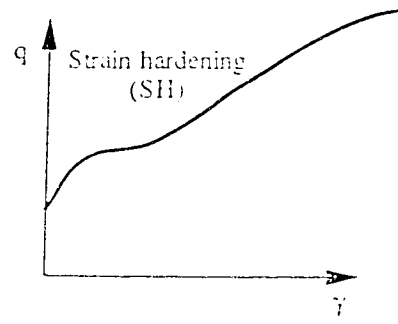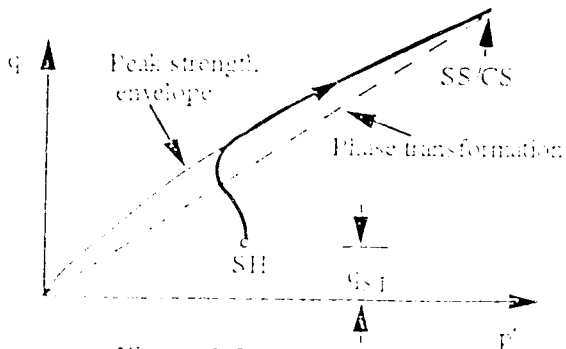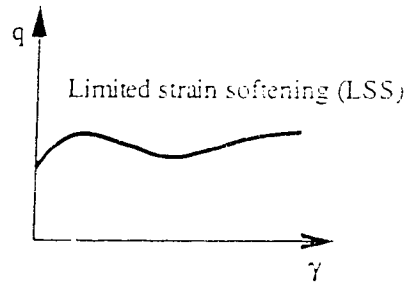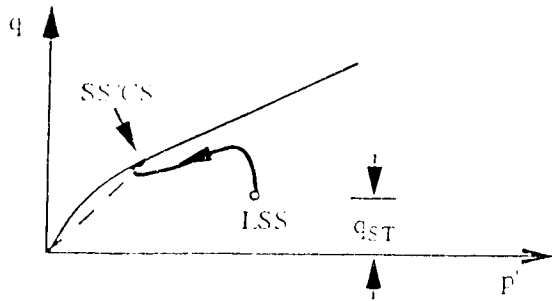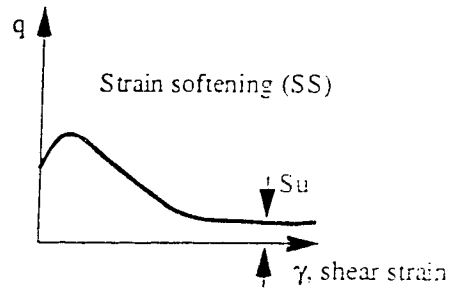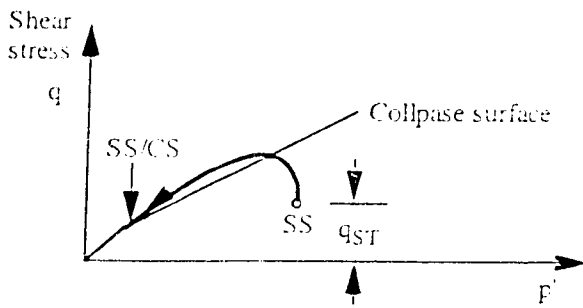
Figure 2.5 Schematic behaviour of a cohesionless soil in response to loading, after Robertson (1994)

29

3.0 Triaxial Testing With Vs Measurement Procedure

3.1 Triaxial Test Description

3.1.1 Test Equipment

A modified Wykeham Farrance loading frame and a modified triaxial cell testing apparatus were used throughout this testing program. The frame modification included a facility to add dead loads to the loading ram to compensate for not having the cell pressure acting on the load head over this ram area. This allowed for isotropic consolidation. The modification to the cell included a special top cap to allow the cell to be assembled with little disturbance to the sample. An internal load cell was used so that friction of the loading ram rod would not be a concern. A schematic diagram of the entire test set up is shown in Figure 3.1.

The loading frame had a variable gearing system to shear the sample in the triaxial cell at a constant strain rate. The gearing is such that the axial strain rate remains constant regardless of the load.

The loading head and base pedestal of the triaxial cell were modified to incorporate bender elements for the measurement of Vs. The initial system used was a single bender element system that protruded 10 mm into the sample at each end (Sasitharan, 1994). As a part of this research a bender element system that was flush mounted in the base and head was developed and incorporated in the platens.

The goal in developing the flush mount system was to be able to measure Vs on undisturbed samples that were obtained by in-situ ground freezing. These samples would be placed in the cell frozen and would not allow the insertion of the benders protruding from the platens. The flush mount system allowed the sample to be placed in the triaxial cell and to thaw under a small confining pressure. Then Vs could be measured after thaw and during consolidation.

Electronic pressure transducers were used for the measurement of cell, back and pore pressures, and a linear voltage displacement transducer (LVDT) was used for measurement of axial displacement, measured from platen to platen. A special volume

change recording device was used to measure changes in volume of the sample during consolidation and drained shearing. Axial load was measured with an internal load cell. All electronic data were recorded by a Fluke 2400 data logging system and stored on files in a IBM XT computer.

3.1.2 Sample Preparation

Sample preparation for the three sands tested employed the moist tamping technique. (Sasitharan, 1994; Pitman, 1993). Moist tamping produces the loosest possible structure for reconstituted soil samples (Ishihara, 1993).

There is some discussion in the literature that the moist tamping technique produces a sample with a fabric that does not represent the true field fabric. However, the technique does produce the loosest structure and gives valuable information for the sand behaviour if the in-situ soil is loose. For the tests carried out on the Alaska sand, the results showed that the loosest structure exhibited highly contractant behaviour, but did not strain soften. Thus it would be expected that this sand would not be susceptible to flow liquefaction.

Some literature suggests that the moist tamping creates a preferred structure. Vaid and Chern (1985) suggest that water pluviation for sample preparation is the most appropriate method for tailings materials that reproduces the in-situ fabric. Work by Skopek (1993) showed dry Ottawa sand prepared by moist tamping did collapse, and that it was the structure that collapsed and caused the pore pressure to increase, not the increase in pore pressure that caused the sand structure to collapse.

With the moist tamping technique the prepared specimen can be very uniform (Sasitharan, 1994) and the fines content will be consistent with that of the input material. From experience in this research, the water pluviation method with a high fines content material like Syncrude sand was found to be difficult to produce a sample that had the same fines content as that of the initial material. This was due to segregation of the fines from the sand matrix in the flask used for deposition.

All the samples of Ottawa and Alaska sand prepared for this test program employed the moist tamping (MT) method. Nine of the 10 tests on Syncrude sand were

31

prepared by moist tamping, and one sample was prepared by the air pluviation (AP) method.

3.1.3 Void Ratio Calculation

Upon sample preparation the void ratio could be accurately calculated from the initial sample dimensions and the soil mass. Changes in the void ratio after preparation were calculated based on the changes in volume during both saturation and consolidation. As pointed out by Sladen and Handford (1987), care must be taken to include the proper volume change during saturation or a serious error can occur in the void ratio calculation. This volume change during saturation cannot be measured directly. One approach is to obtain this by assuming an elastic response which produces the elastic solution as;

$$\varepsilon v \: / \: \varepsilon a = 3 \qquad\qquad\qquad (22)$$

where; εv = volumetric strain (%)
εa = axial stain (%)

This can be used to compute the volumetric change from the axial strain during the saturation. This, however, assumes elastic conditions during saturation and, as pointed out by Sladen and Handford (1987), this tends to underestimate the true volume change for Syncrude sand.

A girth belt around the centre of the sample was used to measure diametric change during saturation and to check the validity of the 3:1 assumption in equation (22). A girth belt is a laminated piece of graph paper which is placed around the sample during preparation and can be seen from outside the cell. An initial reading of the circumference is recorded at preparation and changes in circumference can be recorded during saturation. This produces the change in diameter which can be assumed to be the change in average diameter of the sample. This is reasonable as there is an isotropic stress condition in the triaxial cell. The sample volumetric change during saturation can be calculated and compared to the axial strain. The girth belt could read the circumference accurately to the nearest 0.5 mm.

32

This method was used successfully on the Syncrude sand samples. It was attempted on the Alaska sand samples but there was an error in reading it. From the Syncrude sand results a ratio of between 4:1 and 5:1 was selected to use in equation (22) as the best value to apply for moist tamped prepared samples. A different value of 2:1 was noted in equation (22) for the Syncrude sand AP sample. The elastic assumption of 3:1 was used for the Alaska sand volume change upon saturation in absence of girth belt measurements.

After preparation, the samples were saturated until Skemptons $\bar{b}$ parameter exceeded 0.95. Then, consolidation proceeded in increments of 50 or 100 kPa. The detailed description of the triaxial test procedure is presented in appendix A.

The void ratio could be calculated by the following;

$$e = \frac{Gs\ (Vinit\ -\ \Delta Vsat\ -\ \Delta Vcons.\ -\ \Delta Vmem.\ cor.) \times \rho w}{Ms} - 1 \qquad (23)$$

where; Gs = specific gravity of the solids

ρw = density of water = $1 g/cm^3$

Vinit = initial sample volume, cm^3

$\Delta Vsat$ = calculated volume change during saturation, cm^3

$\Delta Vcons$ = measured volume change during consolidation, cm^3

$\Delta Vmem.\ cor.$ = membrane correction in volume due to penetration, cm^3

Ms = mass of solids, g

As pointed out by Vaid and Negussey (1984) the membrane penetration into the soil voids must be taken into account in the calculation of the void ratio. They suggest a value of $0.0048\ cm^3/cm^2$ per log cycle of effective confining stress for Ottawa sand with a mean grain size (D_{50}) of 0.35 mm. Sladen and Handford (1987) suggests a value of $0.0015\ cm^3/cm^2$ per log cycle of effective confining stress for their test on Syncrude sand. This work used $0.0045\ cm^3/cm^2$ per log cycle of effective confining stress for Ottawa, Alaska and Syncrude sands. The D_{50} of the Alaska sand and Syncrude sand is 0.12 mm and 0.17 mm, respectively. Thus the Ottawa sand membrane correction is not entirely appropriate for these two sands. However, the membrane correction has only a

33

slight effect on the final void ratio calculation and so assuming 0.0045 instead of 0.0015 for Syncrude sand only affects the calculated e by ±0.003.

3.1.4 Monotonic Undrained Loading

Most of the tests for all three sands in this test series were tested in monotonic undrained shear compression loading at a constant strain rate. Samples were prepared by moist tamping as described in Section 3.1.2 and consolidated isotropically to the desired effective confining stress level between 50 and 450 kPa. Upon reaching the desired consolidation stress level the back pressure was locked off and the sample was sheared undrained. The strain controlled test was at a constant strain rate of 0.15 mm/min.

The undrained test is a constant volume test. The void ratio does not change. Net contraction or dilation of the sample is determined by the increase or decrease in pore pressure respectively during shearing.

The stress path of undrained loading was found by Sasitharan (1994) to be the same for the case of a drained constant volume stress path for the same void ratio. However, the moist tamped prepared samples tested in undrained loading only give information about the ultimate steady state at low stress levels due the decrease in effective stresses. Thus some drained tests were undertaken to obtain USS information for Syncrude sand at higher stress levels.

3.1.5 Monotonic Drained Loading

A total of four drained shear compression loading tests were carried out on samples of Syncrude sand. The samples were prepared with moist tamping as describe in Section 3.1.2. They were consolidated isotropically to the desired effective consolidation stress level between 50 and 450 kPa. They were then sheared at a constant strain rate of 0.15 mm/min. under full drainage. The volume change during shear was recorded on the computer by the volume change device along with all the other electronic instruments. The pore pressure was kept constant at the value necessary to maintain saturation. This was ensured by a slow test strain rate to allow the pore pressure generated during shear to fully dissipate.

During drained loading the void ratio is changing and can be calculated with the measured volume change data obtained by the volume change device. The stress path is a straight line at a 3 q to 1 p' slope.

3.1.6 Shear Wave Velocity Measurement

3.1.6.1 Equipment

With the introduction of bender elements it is now possible to measure Vs using a variety of geotechnical laboratory equipment. The bender element offers an inexpensive and simple method to measure Vs in the laboratory tests.

The equipment used in this study consisted of piezoceramic bender elements (see Section 2.3.1.1), a Wavetek 148 A -20 MHz. AM/FM/PM generator, a Kistler 5004 Dual mode Amplifier, a Philips PM 3365A 100 MHz. 100MS/s oscilloscope and a Hewlett Packer HP Color Pro pen plotter. A schematic of the Vs system is shown in Figure 3.1.

The bender element either protrudes into the sample or has its tip flush mounted at the bottom of the sample depending on the system used. After each stage of consolidation is complete, the top bender element is excited with a ±15 volt dc, 20 hertz square wave by the Wavetek wave generator. This causes the cantilever portion of the bender element which is in direct contact with the top of the soil sample to move back and forth producing a transverse (shear) wave in the sample. This wave travels the length of the soil sample until it is received by the base bender element. This bender element is connected to the Kistler dual mode amplifier which amplifies the signal for display on the oscilloscope. Both waves are displayed on the oscilloscope using the average of 8 to 16 of the wave forms. Using the first pulse arrival method the travel time (Δt) in seconds can be obtained from the oscilloscope wave traces. A typical oscilloscope output trace is shown in Figure 3.2. This shows both the generator square wave and the received shear wave. The Δt is the time difference between the two waves, which is marked on Figure 3.2. From the travel time of the shear wave and the known sample height, the Vs can be calculated. This oscilloscope display can then be drawn using the Hewlett Packer plotter. All test data for shear waves were recorded on hard copy plots.

The reproducibility of one wave was very high. If the machine was shut off and the whole process repeated, an identical wave form would appear. However, in different tests the reproducibility of Vs for a similar void ratio and effective stress condition was found to be up to ±7.5 m/s.

The method used in this study to obtain Vs was simple to set up and a large number of test results could be quickly obtained.

3.1.6.2 Protruding Benders

Originally bender elements were aligned to produce shear waves in soil samples by protruding the bender element some 10 mm into the reconstituted sample. The remainder of the bender element length, 20 mm or so, is rigidly attached to the base and head plate of the laboratory equipment to form a cantilevered bender system.

The protruding bender element system used in this research was the system developed by Sasitharan (1994). He used protruding bender elements of dimension 31.8 mm long × 12.5 mm wide × 0.05 mm thick (1.25"× 0.5" × 0.020") installed in the base and head of the triaxial cell. A sketch of the system after Sasitharan (1994) is shown in Figure 3.3.

The benders elements were first coated in a waterproof epoxy to prevent electrical shorting while in contact with pore water. Alignment of the two bender elements in the vertical plane was very important in order to generate and receive a clear shear wave. The travel length of the shear wave displayed on the oscilloscope was taken to be the tip to tip distance of the bender elements. Thus the Vs in m/s was calculated as follows;

$$Vs = (Hcurr. - b) / \Delta t \qquad (24)$$

where, Hcurr. = Current soil sample height, m
        b = total protrusion of the 2 benders, m
        Δt = time of travel of shear wave from oscilloscope in seconds

3.1.6.3 Flush Mount Bender Element System

The flush mount bender element system was designed for this research based on work by De Alba (1993). He showed that the bender elements could be set back in the loading head and base of a triaxial cell system and still produce and receive shear waves in the soil sample. The coupling of the soil and the bender elements was through a flexible membrane window. An array of four bender elements was used as both shear wave generators and receivers. The soil sample in the triaxial cell was placed on top of the four array bender holder with only a flexible membrane separating the soil and the bender element array. The tips of the bender element were within 0.5 to 1 mm of the ends of the soil sample.

Since this membrane was very thin and the bending array was strong the shear wave would still be transferred to the soil, travel through the length of the soil and be received by the bender array at the other end. Again by viewing the generating and received waves on the oscilloscope, the travel time of the shear wave could be calculated using the first pulse arrival method. Since the length of travel is known, the shear wave velocity can be calculated. Sketches of the four bender array and its insertion into the loading head and base are shown in Figure 3.4.

This system uses a PVC chamber to hold four bender elements wired together in series. Each bender element was 25.4 mm long × 6.3 mm wide × 0.05 mm thick (1.0" × 0.25" × 0.02") mounted in cantilever with epoxy at their base. A silicon window of 5 mm (0.2") thickness topped the benders and kept the tips in contact with the soil. A four bender array was used to increase the output and input vibration as the entire flexible window vibrated. This created and received the shear wave.

In order to withstand the large compressive forces generated in triaxial testing the inside of the PVC was filled with silicon oil. This was a non-conductive oil so that electrical shorting of the bender elements would not be a problem. The PVC holder was then installed into the head and base of the triaxial cell as shown in Figure 3.4.

The V_s is calculated as follows;

$$Vs\ (m/s) = Hcurr./\ \Delta t \tag{25}$$

where; Hcurr. = current height of sample, m

   Δt = time delay of shear wave from oscilloscope, seconds

3.2 Materials Tested

In this research three different cohesionless soil materials were tested. These materials were Ottawa sand (OS), Alaska sand (AS), and Syncrude sand (SS). Grain size distribution curves for these three sands are shown in Figure 3.5. A short description of each material follows.

3.2.1 Ottawa Sand

Ottawa C109 sand from Ottawa, Illinois was used in this study. Ottawa sand is a uniformly graded, rounded to sub rounded, clean quartz sand. The soil has a specific gravity of 2.67 and maximum and minimum void ratio of 0.82 and 0.50, respectively, using ASTM D2049. The mean grain size, $D_{50} = 0.35$ mm. A gradation curve of the OS is shown in Figure 3.5.

The Ottawa sand is investigated in this research in order to add to the data of Sasitharan (1994) who performed similar triaxial testing with Vs measurement on loose and dense samples. The Ottawa sand is a clean uniform rounded sand which is a type of material that is highly susceptible to liquefaction problems and thus of interest in investigating for the potential for flow liquefaction.

Scanning electron microscope (SEM) analysis for Ottawa sand is presented and discussed in Section 4.5.

3.2.2 Alaska Sand

Alaska sand is an angular sand obtained from a marine tailings deposit in the state of Alaska. The deposit is believed to be from an old mine waste area and has been in a marine environment for up to 70 years.

The Alaska sand used in this test series was delivered to the University of Alberta from the mine site. A total of 9 samples obtained from the drilling and sampling program were chosen from specific elevations. Of these samples, 6 were screened and the material passing the #4 (4.76 mm) sieve was mixed together to form a testing batch.

A grain size curve of AS is shown in Figure 3.5. The mean grain size, $D_{50} = 0.12$ mm. The fines content averaged 31.7% passing the #200 (74μm) sieve. The soil has a specific gravity of 2.90 and maximum and minimum void ratio of 1.78 and 0.70, respectively, using ASTM D2049. The maximum void ratio appears very high. The ASTM standard suggests that this method is not reliable for material with a fines content of greater than 5%; and thus the higher than normal maximum void ratio for this material.

SEM analysis was carried out on a sample of the Alaska sand this is presented and discussed in Section 4.5.

The interest in testing this Alaska sand material stems from a practical application of the liquefaction analysis procedure. During a field investigation of this sand deposit the SCPT data was interpreted to give conflicting information. The CPT qc data was interpreted to show that the sand was "very loose" using existing correlations and thus susceptible to flow liquefaction. The SCPT produced Vs data was interpreted to show that the sand was "dense" using existing correlations and hence not susceptible to flow liquefaction.

Thus the interest in testing this material in the framework of Vs measurement within CSSM was to investigate this material and attempt to provide reasons for this conflicting information interpreted from the two in-situ tests.

3.2.3 Syncrude Sand

Reconstituted tests on Syncrude sand were preformed with material obtained as a bulk sample from the beach material at the Syncrude tailings facility. Syncrude sand is a sub-angular uniform tailings sand. The Syncrude sand is a tailings by-product of the extraction of synthetic oil from the Alberta oilsands.

The grain size curve is shown as SS in Figure 3.5. The mean grain size, $D_{50} = 0.17$ mm. The average fines content for the material tested in this research was 12.4% passing the #200 (74μm) sieve. This sand has a specific gravity of 2.62 and maximum and minimum void ratio of 1.04 and 0.61, respectively, using ASTM D2049.

SEM analysis for Syncrude sand is presented and discussed in Section 4.5.

As part of Phase I of the CANLEX project a section of the Syncrude tailings facility was chosen as a test site to investigate loose cohesionless material under high overburden stress. CANLEX investigated this deposit to locate the loosest zone of material at depth. One of the goals of CANLEX was to use ground freezing to obtain high quality undisturbed samples of this loosest material that existed over a depth of 27 to 37 meters. These samples would be tested at number of different university laboratories.

In order to characterize the Syncrude sand and compare data obtained from the undisturbed sample results, laboratory tests were carried out on reconstituted samples. In-situ test such as SPT and SCPT were also preformed at the test site.

This research carried out tests on a number of reconstituted samples of Syncrude sand for USS data and developed the e-p'-Vs relationship for the sand. The USS results from this study were combined with test results from other laboratories testing reconstituted samples using other preparation methods and using different testing equipment.

In addition to typical field investigation data the field data obtained from CANLEX included accurate measurement of void ratio with depth in the zone from 27 to 37 meters. The void ratio was calculated from the undisturbed frozen core samples. This data was coupled with the in-situ Vs measurement and was compared directly to the laboratory data.
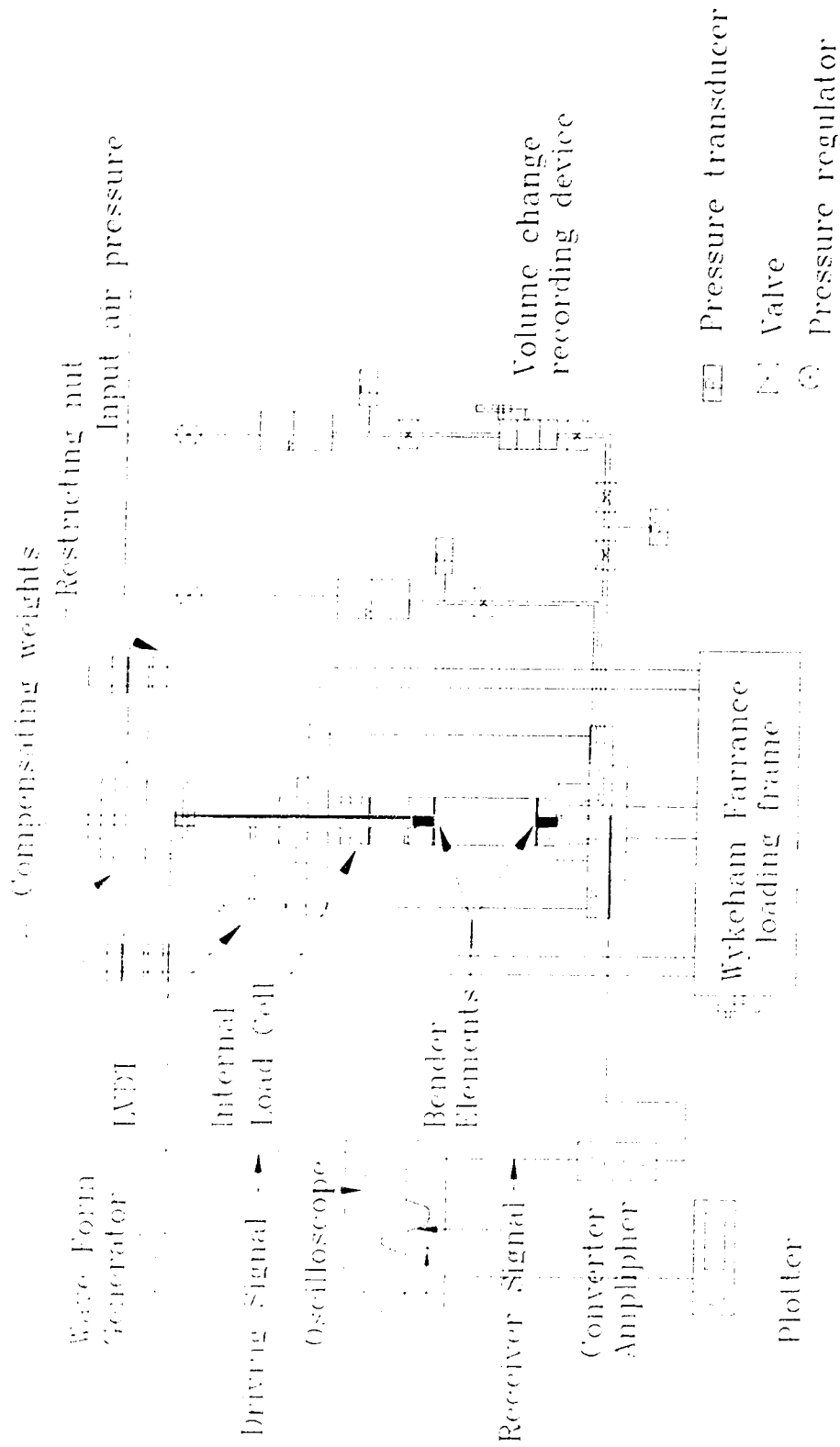
Figure 3.1 Schematic diagram of the testing apparatus used in this research.

41

Generator Wave

Received Shear Wave

Δtime, (μseconds)

First pulse arrival of shear wave
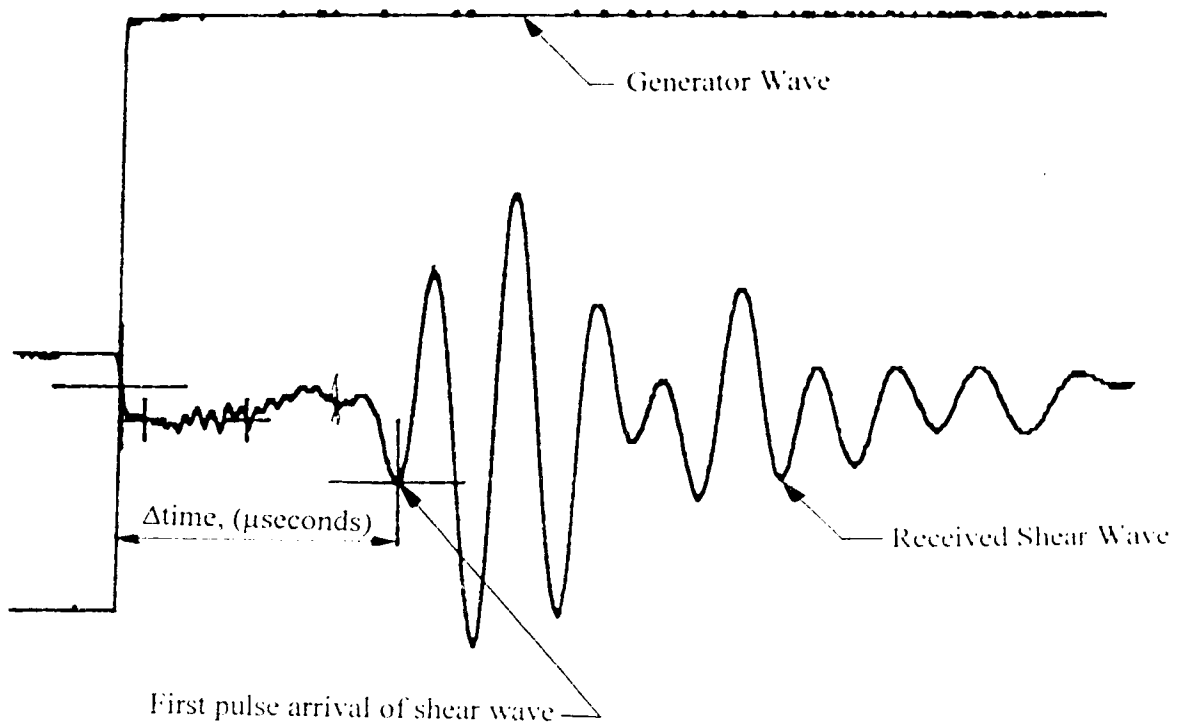
Figure 3.2 Typical plot of laboratory shear wave during consolidation in triaxial testing

42

Bender wires

Load head

Porous stone

Soil

63.5 mm

Protruding
Bender
Element

Silicone

Epoxy

Porous stone

Base
pedestal

Bender wires
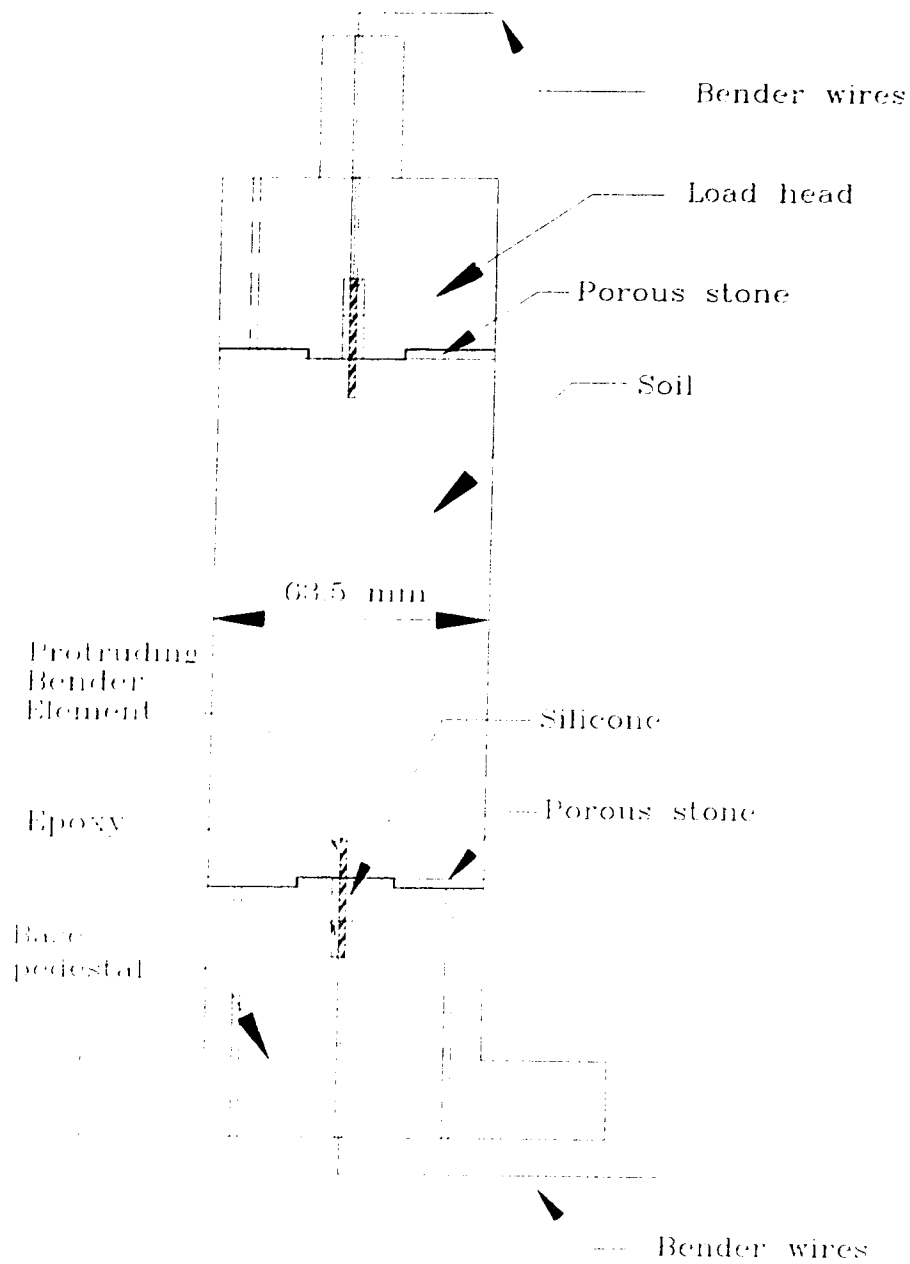
Each bender element
3.2 mm L x 12.5 mm W x 0.5 mm t

Figure 3.3 Protruding bender element system in triaxial cell head and base after Sasitharan (1994).

43
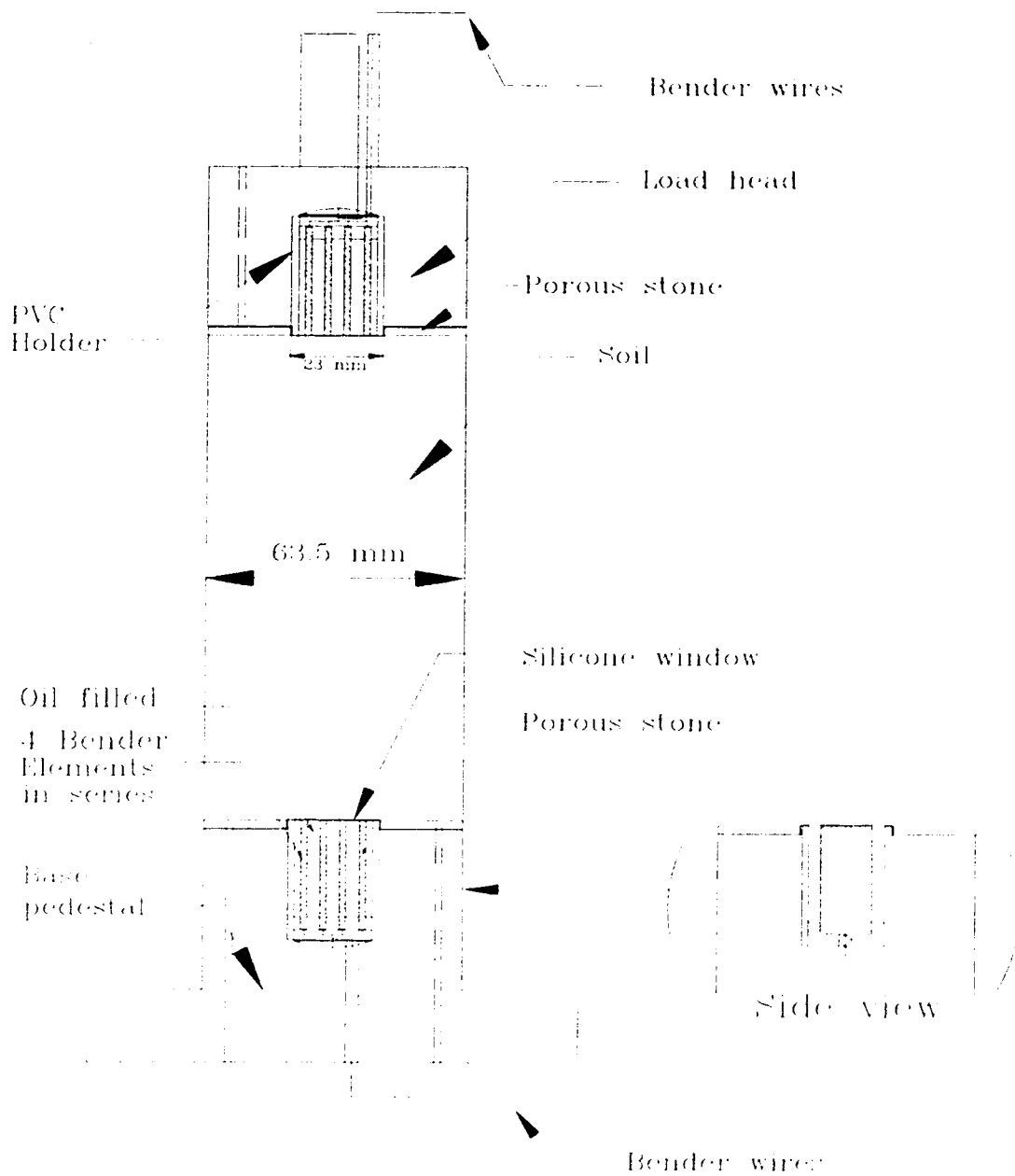
Figure 3.4 Flush mount bender element system in triaxial cell head and base
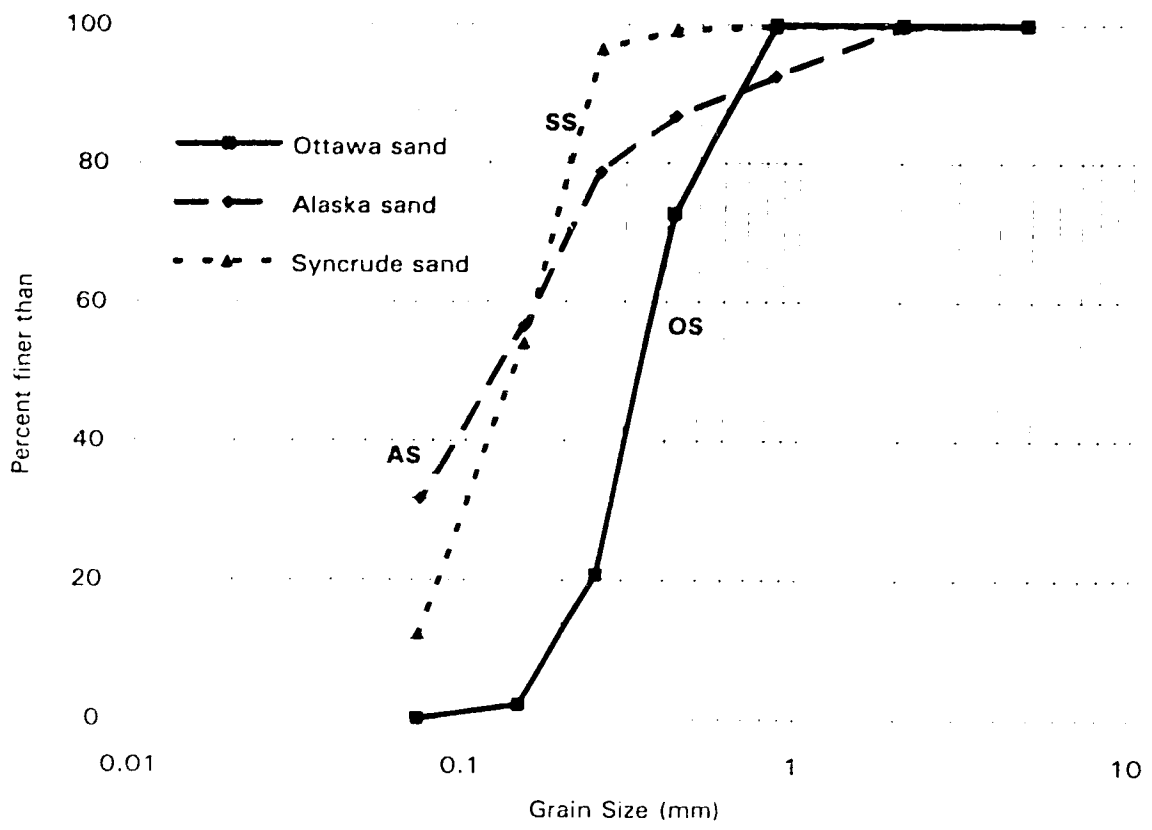
Figure 3.5 Grain size distribution curves for Ottawa, Alaska and Syncrude sands.

4.0 Test Results

The test results will first be presented for the Vs measurement during consolidation in order to develop an e-p'c-Vs relationship for each of the three sands. Then, the shear loading test results will be presented and the USS parameters given for each sand. Next, the measurement of the Vs at the USS will be investigated in order to confirm the e-p'-Vs relationship for anisotropic stress states. This will also show that the e-p'c-Vs relationship is also an e-p'-Vs relationship.

Each test performed is given an identification string to describe it. An example string is SS-340-T4-CU which stands for; SS = Syncrude sand, 340 = the isotropic consolidation stress at start of shear in kPa, T4 = test 4 in the series and CU is consolidated undrained test. Other abbreviations are: OS = Ottawa sand, AS = Alaska sand, CD = consolidated drained test, and AP = air pluviated.

4.1 Consolidation Vs Measurement Results

The results of Vs measurements during consolidation were considered separately for each material tested. The results provide a sand specific e-p'c-Vs relationship for each sand which is described in the following sections.

4.1.1 Ottawa Sand Vs Results

A total of six tests were carried out on Ottawa sand with Vs measurements during isotropic consolidation. The samples were all prepared by the moist tamping technique to ensure a very loose structure. Table 4.1 gives a summary of the test data for e, p'c and Vs for this present study.

Data from a previous study by Sasitharan (1994) was compiled with the data from this study. A total of twelve tests were carried out in the study by Sasitharan (1994) and Table 4.2 provides a summary of the data in terms of e, p'c and Vs. Together, all test data from Tables 4.1 and 4.2 were used to develop the e-p'c-Vs relationship for Ottawa sand.

Data from Sasitharan (1994) used both moist tamping and water pluviation for sample preparation. All this data was considered in developing the e-p'c-Vs relationships.

Figure 4.1 shows all the data from both studies in terms of Vs against e and Figure 4.2 shows the data in terms of Vs against p'c. All the data from the present study and only selected data from the previous study are shown in the Figure 4.2 to illustrate the trends.

It can be seen from both figures that Vs changes with changes in both e and p'c. Of note in Figure 4.1 is that there are three different trends for the different void ratio ranges of very loose, medium and dense. Also shown in Figure 4.2 are lines of constant e predicted by the equation for Ottawa sand that will be developed later in this section. These lines show what the relationship would be between Vs and p'c if e was not changing during consolidation. A slight deviation of the data from the line of constant e is expected since e changes during consolidation (see Figure 4.4).

In order to compare the three independent measurements the laboratory measured Vs was normalized with the stress state at which the measurement was made. Figure 4.3 shows a plot of normalized shear wave velocity (Vs1) against e. The normalization was carried out using equation (9) which is repeated below

$$Vs1 = Vs * (100/p'c)^n \qquad (9)$$

The Ottawa sand data was normalized with the exponent $n = 0.266$. This value of n was chosen by observing the normalization of the data and the linear regression coefficient (r^2). The value of r^2 is a measure of the fit of the data to the linear regression. When the r^2 was plotted against the exponent n, a optimum value of $n=0.266$ was noted at the highest value of r^2 of 0.93.

Figure 4.3 shows results for samples prepared using both MT and WP over a large range of void ratio. It is likely that these samples had different fabrics. However, the linear regression through all the data fits the dense samples as well as the very loose samples. This implies that fabric plays only a minor role in the Vs1 - e relationship

It was also necessary not to consider some Vs data measured at a consolidation stress level of 50 kPa and less. Both this testing and data from Sasitharan (1994) had measurements of Vs at the p'c = 50 kPa stress state. Some of this low consolidation stress data did not fit with the high consolidation stress data. This was also noticed by Hardin and Richart (1963) in their development of an e-p'-Vs relationship. They suggested that there are two different relationships between e-p'-Vs, one for p' below 100 kPa and one for p' above 100 kPa. Thus the p'=50 kPa Vs measurements were not included in the development of the e-p'-Vs relationship. A second reason for this is that in this triaxial testing the sample at p'c = 50 kPa may not be at exactly 100% saturation

(i.e. $\bar{h}$=0.95). However, for the consolidation state above p'c = 50 kPa, saturation should

be very close to 100% (i.e. $\bar{h}$=1.00).

From the Vs1 - e data in Figure 4.3 linear regression was used to develop the Ottawa sand Vs1 - e equation based on all the data gathered. This relation is expressed as;

$$Vs1 = \{381-(259 \cdot e)\} \tag{26}$$

Upper and lower bound values were computed to fit most of the data which was slightly scattered and these relationships can be expressed as.

$$Vs1 \text{ upper} = \{390-(259 \cdot e)\} \tag{27}$$

$$Vs1 \text{ lower} = \{370-(259 \cdot e)\} \tag{28}$$

These upper and lower bounds represent a variation in Vs1 of ±2.9% from the average at the same e.

The average Ottawa sand equation for Vs1-e (26) was combined with the normalization equation (9) to give the average e-p'c-Vs equation as,

$$Vs = \{381-(259 \cdot e)\} \cdot (p'c/100)^{0.266} \tag{29}$$

Figure 4.4 shows all the data in the form of a consolidation plot of e against log p' with contours of Vs based on the above Ottawa sand equation (29). This plot shows the range of e and p' over which data was gathered. The plot also shows the consolidation data for all the tests on Ottawa sand. Again three different void ratio ranges are covered which are produced by two different preparation methods. Also included is the USSL based on the shear loading tests which are described in a later section. The moist tamped very loose samples almost all have consolidation states above the USSL. The medium and dense water pluviated sample are all below the USSL. The consolidation data in Figure 4.4 shows that the Ottawa sand has very flat consolidation curves which indicate very low compressibility. Note that in Figure 4.4 the Vs contours are displayed over a slightly larger range of both e and p' than measured in the tests. This is an extrapolation and will be discussed later.

Figure 4.5 shows the consolidation of five individual typical tests, two from the present study, and three by Sasitharan (1994). Each consolidation point is marked with its measured Vs in m/s. The results show how well the Vs data for each consolidation point matches the contours. A good agreement is generally noted.

Figure 4.6 shows the Vs measured in all the tests plotted against the Vs predicted by the Ottawa sand equation (29). A good agreement can be seen for most of the data.

Sasitharan (1994) gave a relationship between e-p'-Vs as;

$$Vs = \{317-(181 \cdot e)\} \cdot (p'/100)^{0.25} \tag{30}$$

which is slightly different from the equation (29) proposed above. However, the Sasitharan (1994) equation was based on only the very loose sample data whereas the relationship presented here is obtained using data from samples at different densities.

4.1.2 Alaska Sand Vs Results

A total of 6 tests were carried out on the Alaska sand. All were isotropically consolidated to between 40 and 352 kPa effective confining stress with Vs measurements made at each stage of consolidation. All samples were prepared using the moist tamping

technique in order to obtain the loosest structure. Table 4.3 gives a summary of the laboratory measured e, p'c and Vs for the Alaska sand.

Figure 4.7 shows the data in terms of Vs against e and Figure 4.8 shows the data in terms of Vs against the p'c. From both figures it is noted that all tests give data over a small range of e, all at the very loose state (0.9<e<1.25). Only one preparation method was employed in these tests and thus a smaller range of e was covered as compared to the Ottawa sand data.

Figure 4.8 also shows lines of constant e predicted by the equation for Alaska sand that will be developed later in this section. From both figures it can be seen that the data shows Vs changing with both p'c and e. Alaska sand is highly compressible which is noticed in the Vs -p'c space (Figure 4.8) as the data tends to cross from one line of constant e to another with increasing p'c.

In order to compare the data, Vs was normalized with p'c using equation (9) and an exponent of n=0.26. The exponent of 0.26 was chosen from the best fit of the data, as explained for Ottawa sand. Figure 4.9 shows the Vs1 against e plot. Linear regression of the data gives the average Alaska sand Vs1- e equation as;

$$Vs1 = \{307-(167 \cdot e)\} \qquad (31)$$

with upper and lower bounds to all the data of equations;

$$Vs1 \text{ upper} = \{312-(167 \cdot e)\} \qquad (32)$$

$$Vs1 \text{ lower} = \{303-(167 \cdot e)\} \qquad (33)$$

These upper and lower bounds represent a variation in Vs1 of $\pm 1.6\%$ from the average at the same e.

The average Alaska sand equation for Vs1 - e (31) was converted into the e-p'c-Vs with the use of equation (9) and gives a relation as;

$$Vs= \{307-(167 \cdot e)\} \cdot (p'c/100)^{0.26} \qquad (34)$$

This is the Alaska sand e-p'c-Vs equation and is used to contour the e - p' diagram with Vs. Figure 4.10 shows this diagram with the consolidation data for all the tests as well as the USSL derived from shear loading tests and described in a later section. The consolidation data show that this sand is highly compressible and that the samples were all prepared very loose of the USS.

Figure 4.11 shows one set of consolidation data with each point marked with the Vs measured during the test. A good agreement between the data and the contours is noticed.

The data for Alaska sand is only available in the very high void ratio range of 0.9 to 1.1, with effective stresses varying from about 50 to 350 kPa. Again the Vs contours were plotted over a range larger than the test data and this is an extrapolation. This will be discussed later.

Figure 4.12 is a plot of all the Alaska sand laboratory measured Vs data against the predicted Vs with the average Alaska sand equation (34). Again a good agreement is observed.

4.1.3 Syncrude Sand Vs Results

A total of ten tests were carried out on the Syncrude sand. Nine of the ten tests were prepared by the moist tamping technique and one test was prepared using the air pluviation technique. Table 4.4 gives a summary of the laboratory data in terms of the measured e, p'c, and Vs. All samples were isotropically consolidated to between 54 and 453 kPa effective confining stress with Vs measurement throughout consolidation.

Figure 4.13 shows all the data in terms of Vs against e and Figure 4.14 shows all the data in terms of Vs against p'c. In Figure 4.13 it can be seen that three zones of the e range were covered for the Syncrude sand. The first zone, where most of the data lies, is for the moist tamping with 5% moisture content and are the very loose samples. For a slightly denser structure one test was moist tamped at 10% moisture content. For the densest structure tested the technique of air pluviation was used.

It can be seen from both the figures that the Vs is changing with both the e and p'c Figure 4.14 shows lines of constant e predicted by the equation for Syncrude sand that will be developed later in this section. A slight deviation of the data from the line of constant e is expected and is seen for Syncrude sand as the material has a very low compressibility.

In order to compare the data, Vs was normalized with p'c using equation (9) and an exponent of n=0.26. The exponent value of 0.26 was chosen from the best fit linear regression much the same as the Ottawa sand procedure. The plot of Vs1 against e is shown in Figure 4.15. The average Syncrude sand Vs1 - e equation was determined from linear regression and can be expressed as;

$$Vs1 = \{311-(188 \cdot e)\} \tag{35}$$

with upper and lower bounds to all the data expressed by the equation as,

$$Vs1 \text{ upper} = \{321-(188 \cdot e)\} \tag{36}$$

$$Vs1 \text{ lower} = \{302-(188 \cdot e)\} \tag{37}$$

These upper and lower bounds represents a variation in Vs1 of ±3.2% from the average at the same e.

The average Syncrude sand equation for Vs1 - e (35) was combined with the normalization equation (9) to give the average e-p'c-Vs equation as;

$$Vs = \{311-(188 \cdot e)\} \cdot (p'c/100)^{0.26} \tag{38}$$

This equation was used to draw contours onto the e log p' plot in Figure 4.16, which shows all the consolidation data for Syncrude sand and the USSL derived from shear loading test that are described in a later section This plot shows the range of e and p'c for all consolidation data. This plot also shows that the consolidation of the Syncrude sand is of low compressibility and that all the very loose moist tamped samples plot above the USSL.

Figure 4 17 shows two different sets of consolidation data with each point marked with its laboratory measured Vs. There is good agreement of the Vs measured in the test with the contours from the equation.

Figure 4.18 shows all the Vs measured data against the Vs predicted by the Syncrude sand equation (38). Again a good agreement is observed.

4.2 Shear Loading Results

After consolidation with Vs measurement, all samples were then loaded in shear either undrained or drained. The results in terms of the USS parameters will be given below for all the materials tested.

4.2.1 Ottawa Sand USS Parameters

A total of five triaxial compression tests were carried out on Ottawa sand which were all isotropically consolidated to between 160 and 361 kPa. The tests were all sheared undrained at a constant strain rate of 0.15 mm/min. All samples were prepared by the moist tamping technique to ensure a very loose structure. Table 4.1 summarizes the e, p', Vs, $\sigma'1$, and $\sigma'3$ at USS for these tests on Ottawa sand.

Sasithara⁻ (1994) provides the results of 7 undrained shear tests on very loose moist tamped samples of Ottawa sand. His results are summarized in Table 4.2. All the data is shown together in Figure 4.19. Figure 4.19a shows the data in e against log p' and 4.19b shows the data in quss against p'uss. These plots are used to determine the USSL. The USS parameters are presented at the end of the section.

Figure 4.20a shows the results of the five tests from this study in terms of q against axial strain and 4.20b shows the change in pore pressure against axial strain. It can be seen that almost all samples reached a peak deviator stress within 0.5% to 1% of axial strain. The change in pore pressure shows a continued increase to about 4-6% of axial strain before levelling off. Three of the tests exhibited a clear strain softening response. Their change in pore pressure rose up to a peak value at between 4 to 6% strain and stayed constant for the remainder of the test. Two tests showed slight strain softening

53

followed by strain hardening. In these tests the change in pore pressure increased slightly at first but ultimately decreased. Consolidation states for the two strain hardening tests are those that are very close to or below the USSL and not above it like those of the strain softening tests.

Figure 4.21 shows the normalized stress paths in terms of q/p'uss against p'/p'uss The normalization follows that suggested by Sladen and Oswell (1989) where the stress state (q,p') is divided by the p'uss. This normalizes out the effect of different void ratios for the different tests. Thus all tests should end at the point of q'uss/p'uss $=$ M and p'uss/p'uss =1.

The USSL can be seen in this plot as a point and the collapse surface can be seen as a line. For Cttawa sand it can be seen that the collapse line has a slope of 1p':0.8q This is the same value for collapse as reported by Sasitharan (1994). This line covers the post peak portion of the undrained stress paths and goes through the USS point

Based on all the results the following USS parameters were determined to describe Ottawa sand;

$$\Gamma = 0.926$$
$$\lambda \, (\log) = 0.0745$$
$$M = 1.2 \, (\phi cv = 30^\circ)$$
$$s = 0.8 \, (\phi' \text{ collapse} \cong 20^\circ)$$

These values are valid over a stress range of p' $=$ 8 to 820 kPa

4.2.2 Alaska Sand USS Parameters

A total of six triaxial compression tests were carried out on the Alaska sand All samples were prepared with moist tamping technique in order to obtain the loosest structure and were isotropically consolidated to between 54 and 352 kPa effective confining stress The samples were all sheared in undrained triaxial compression at a constant strain rate of 0.15 mm/min. Table 4.3 summarizes the e, p', Vs, $\sigma'1$ and $\sigma'3$ at USS for all tests.

Results of the six tests on Alaska sand are shown in Figure 4.22a in the e against log p' plot and in 4.22b quss against p'uss plot. Also shown on the Figure 4.22a plot is the consolidation data. It can be seen that all samples were consolidated above the USSL. These plots are used to determine the USS parameters which are given at the end of the section.

In AS-54-T1-CU there was an unknown error in the void ratio calculation during the experiment. This data point is included on the e - log p' plot (Figure 4.22a) with a question mark. The results from this test are not shown in the remaining plots nor is it used in the determination of the USSL.

Figure 4.23a shows the deviator stress against axial strain and 4.23b shows the change in pore pressure against axial strain for the six tests. It can be seen that all tests reached their peak deviator stress at about 1% axial strain. The tests at the lower effective confinement showed only very slight strain softening response and as the confinement increased a slight strain hardening response was noticed. The change in pore pressure shows a continual rise up to about 4-6% axial stain where it levels off. This pore pressure increase in an undrained test indicates contractive behaviour.

Normalized stress paths are shown in Figure 4.24 and show that all tests converge on the same USS point. This plot shows the PT which occurs at a mobilized friction angle of 32.3° and the USS which occurs at a mobilized friction angle of 36.5°.

The very loose Alaska sand samples showed a highly contractive response, but showed no strain softening behaviour. All samples reached a peak shear stress and then upon further shear sustained that shear strength. This cohesionless material did not exhibit strain softening response in any of the tests presented here and thus is not susceptible to collapse behaviour at least within the stress and void ratio range tested.

The results give the USS parameters as;

$$\Gamma = 1.485$$
$$\lambda (\log) = 0.270$$
$$M = 1.48 \ (\phi cv = 36.5 degrees)$$
$$PT \ at \ M=1.3 \ (\phi p_T = 32.3°)$$

These vaiues are valid over a range of p'=30-150 kPa.

No value has been given for the slope of the collapse surface (s), since none of the samples showed a strain softening response. However, the samples showed a well defined phase transformation (PT) point for contractive to dilatant behaviour.

SEM photo analysis was carried out on a frozen sample of Alaska sand obtained after shearing at the USS. See section 4.5 for a detailed discussion of the Alaska sand SEM.

4.2.3 Syncrude Sand USS parameters

A total of ten triaxial compression tests were carried out on the Syncrude sand. Nine of the ten tests were prepared by the moist tamping technique and one test was prepared using the air pluviation technique. All samples were isotropically consolidated to between 54 and 453 kPa effective confining stress. Seven of the samples were sheared undrained and four were sheared drained, all at a constant strain rate of 0.15 mm/min. Table 4.4 summarizes the e, p', Vs, $\sigma'1$ and $\sigma'3$ USS for all tests.

As a part of the CANLEX project, testing by other university laboratories was carried out on the same bulk samples of Syncrude sand. A summary of the results by others is given in Table 4.5.

Tests at the University of British Columbia (UBC) were prepared using both WP, and AP. Tests at the Centre for Cold Oceans Resources Engineering (C-CORE) were prepared by AP. All tests were undrained and some were carried out using triaxial compression, triaxial extension and simple shear.

The results of the undrained and drained triaxial compression tests from this study along with selected test results from the CANLEX (1994) information are shown together in Figure 4.25 in e against log p' plot and in Figure 4.26 in quss against p'uss plot. Only compression and simple shear tests were used in these plots

Figure 4.27a shows the q against axial strain and 4.27b shows the change in pore pressure against axial strain for the undrained tests from the present study. All these samples except SS-437-T8(AP)-CU reached a peak shear strength in the first 0.5% to 1% axial strain. Then they showed a large strain softening response in which shear strength dropped to its low value at ultimate steady state. SS-437-T8(AP)-CU, which was consolidated below the USSL, showed a slight strain softening followed by strain hardening.

Figure 4.28a shows the q against axial strain plot and 4.28b shows the change in volume against axial strain plot for the drained tests from the present study. The drained tests all rose very slow in q against axial strain space and took up to 20% axial stain to reach the peak shear resistance. During this the volume change showed continual contraction until it reached a constant value at the USS. It appears that at about 20% axial strain the tests reached a constant q and constant volume which is the USS.

Figure 4.29a shows the normalized stress paths for the undrained tests. The USS point can be seen as well as the clearly defined collapse line of the undrained tests. The slope of the collapse line is s = 0.9 taken through the USS point and is similar to the collapse line of s= 0.8 for Ottawa sand. This collapse line is very important and as shown by Sasitharan (1994) represents a state boundary for the sand. If a stress path tries to cross this state boundary a collapse is expected. This collapse line for Syncrude sand is the equivalent of a mobilized friction angle of $\phi'm \cong 22°$.

Figure 4.29b shows an expanded view of the USS point and the collapse line. Also shown are the normalized drained stress paths which all rise up from a low p'/p'uss value to the USS point of (1,M). Because they start so low in p'/p'uss they do not plot clearly as individual tests on the normalized stress path. The collapse line can be seen to occur at a mobilized friction angle much less than the USSL with M = 1.3.

From all the data in figures 4.25, 4.26 and 4.29 the following USS parameters were determined for Syncrude sand.

$$\Gamma = 0.928$$
$$\lambda \log = 0.0637$$
$$M = 1.31 \; (\phi'm = 32.5°)$$

$$s = 0.9 \quad (\phi'm \cong 22°)$$

These values are valid over the range of p'= 6 to 800 kPa.

There exists a possibly of a break in the USS line as the p' increases over about 800 kPa as suggested by data from Been *et al.* (1991). They showed test results on Leighton Buzzard sand and Erksak sand that displayed a definite change in slope of the USSL in e against log p' plot for a p' greater than 1000 kPa. A linear regression was assumed in the interpretation of this data since no tests had given information beyond the break in the USSL.

4.3 Vs Measurement at USS

After shear loading of most specimens to large strain in order to determine the USS parameters as outlined above, a Vs measurement was taken and recorded with the stress condition at USS. This data is discussed below for each material and confirms the equation of e-pc'-Vs. It also helps to extend the range of validity of the measured data.

4.3.1 Ottawa Sand Vs at USS

Table 4.1 summarises the Vs measured and individual stress conditions at USS for tests on Ottawa sand for this present study. Table 4.2 summarizes the Vs measured and p' at USS for the tests on Ottawa sand after Sasitharan (1994).

The (Vs)USS data from this study was normalized with the following individual stress equation;

$$Vs1 = Vs *(100/\sigma'1)^{n/2}*(100/\sigma'3)^{n/2} \tag{39}$$

This is to compare data at USS in an anisotropic stress state to the normalized isotropic consolidation data. The two individual stress exponents were assumed to be equal and thus n/2 was used. For Ottawa sand, n=0.266. The (Vs1-e)USS data is shown in Figure 4.30. Also shown is a line representing the average Ottawa sand Vs1 - e equation (26) based on an isotropic consolidation state.

The data from Sasitharan (1994) did not give the individual stress states and the (Vs)USS was normalized with the (p')USS using equation (9). There is only a small error introduced by this normalization. Also only four tests were available to show Vs at USS.

The USS data appears to agree with the best fit line for the Ottawa sand consolidation equation. However, the data exists only over a small range of e. This does show that the Ottawa sand e-p'-Vs equation appears to be valid for the anisotropic stress state.

4.3.2 Alaska Sand Vs at USS

Table 4.3 gives the Vs measurement data for the Alaska sand at the USS as well as the stress conditions. The (Vs)USS was normalized with the two individual stress method using equation (39) and an exponent of n/2. For Alaska sand, the exponent n=0.26. Figure 4.31 shows the (Vs1- e)USS data as well as the line representing the average Alaska sand Vs1-e consolidation equation. A good agreement is seen between the Vs data at USS and this line. Thus the Alaska sand e-p'-Vs equation appears to be valid for the anisotropic stress case.

4.3.3 Syncrude Sand Vs at USS

Table 4.4 gives the Vs measurement data for the Syncrude sand at USS as well as the stress conditions. The (Vs)USS was normalized with the two individual stress method using equation (39) and an exponent of n/2. For Syncrude sand, the exponent n= 0.26. Figure 4.32 shows the (Vs1-e)USS data as well as the line representing the average Syncrude sand Vs1 - e consolidation equation. A good agreement is seen between the Vs data at USS and this line. Thus the Syncrude sand e-p'-Vs equation appears to be valid for the anisotropic stress case.

4.3.4 Syncrude Sand Field Vs and e Data

As a part of the CANLEX project, in-situ Vs data was gathered during the field investigation using SCPT. In the same area as that the SCPT was carried out, ground freezing was used to obtain high quality undisturbed Syncrude sand samples from depths

59

of between 27 and 37 meters. Very accurate void ratios were calculated from density measurements on the frozen samples with precise depth location. These void ratios were matched with the in-situ Vs measurements by matching the depths at which the measurements were taken. This resulted in field Vs and e data that could be normalized with equation (39) using n=0.26. This Vs1 - e field data is compared to the laboratory data in Figure 4.33, which shows data points from the field as well as a line representing the average Syncrude sand e-p'-Vs consolidation equation.

A value of Ko was assumed in order to calculate the p' stress state from depth and soil bulk density data. From preliminary pressuremeter tests it was assumed to be in the range of Ko = 0.5 to 0.8. The locations of the data points are sensitive to the value of Ko. A value of 0.75 was found to give the data good agreement in terms of Vs1 - e for most of the data.

One note for this plot is that the Vs measurement hole was some 10 meters away from the hole where the frozen samples for void ratio determination were obtained. Thus there is possibly some error in assuming the two measurements could be correlated

4.4 General Comment on e-p'-Vs Relationship

Compiling the e, p'c and Vs data to obtain a relationship appears to be a reasonable method that worked for the three different materials investigated. This relationship was confirmed with data at the USS and thus for an anisotropic stress state. The preliminary in-situ data for the Syncrude sand was also found to give agreement to the relationship for Syncrude sand.

Thus it should be reasonable to extend the e-p'-Vs over limits slightly in excess of that which the data was gathered to develop it. This has been done on the previously presented e against log p' plots with Vs contours. The e, p' and Vs data for Alaska and Syncrude sand does not cover much of the e against log p' space and yet Vs contours are shown over the length of the diagram. This appears to be reasonable because of the fact that the e-pc'-Vs equations are valid for general stress states and can be represented in the form of e-p'-Vs and that the extension in any of the variable e, p' and Vs is kept to a minimum.

4.5 Scanning Electron Microscope Results

A series of scanning electron microscope (SEM) photos were taken of the sample AS-250-T7-CU after the sample was shear undrained to USS. The sample was frozen without disturbance and sections were cut out in order to perform SEM analysis. For a detailed description of this procedure to obtain the soil section for SEM photos see Pitman (1993). This analysis was carried out to make some observations on the fabric of this material.

Photos from a previous study on Ottawa sand by Sasitharan (1994) and a study on Syncrude tailings sand by Küpper (1991) are also include here for discussion of these materials fabric. The SEM photos for the Syncrude samples have been taken from field samples at the Syncrude tailings facility and a detailed description of this procedure for these SEM photos is described in detail in Law (1991).

SEM provides photos of the soil sample to scales great enough to view the fabric and make some observations on the grain to grain contacts, the mixing of the soil's constituent particles and the location of the fines in the overall soil matrix as well as providing some basic mineralogy analysis. The information obtained from SEM can be used in addition to the geotechnical laboratory test results to help make geotechnical engineering decisions about the material in question.

A series of two photos of Ottawa sand is shown in Figure 4.34 for very loose Ottawa sand at the consolidation state, and two photos are shown in Figure 4.35 for very loose Ottawa sand at the USS. Both photos are taken from Sasitharan (1994). The Ottawa sand can be seen in these photos to have rounded to sub-rounded sand grains with little to no fines in the soil matrix. The packing of the grains shows a high porosity and hence high void ratio. Uniformity of the grain size of Ottawa sand can be seen in the photos. Grain to grain contacts are clearly observed.

Figure 4.36 shows the six photos taken for the Alaska sand sample at 45 degrees to the horizontal axis of the sample. Figure 4.37 shows the six photos taken at the 90 degrees to the horizontal and Figure 4.38 shows the four photos taken at the horizontal axis of the sample. The magnification of the soil particles varies in the photos from 27.5

times for the 400 μm scale to 2750 times for the 4 μm scale. The scale is marked in the lower left corner of each photo.

The SEM results showed that the sample consisted mainly of a mix of siliceous sand particles, clay mineral particles, and calcitic material in the form of sea shells. The mineralogy break down by the SEM showed about 42% siliceous mineral, 25% iron mineral, 13% calcite mineral and some smaller quantities of the other minerals. The siliceous material would be present as both quartz particles and as clay particles.

Photos with a scale reading of 400 μm, 200 μm and 100 μm show the matrix of the material as a mix of the three main constituents. One individual material could not be seen to dominate the soil matrix of this sample. The orientation of the sand particles was very hard to pick out of the photos because of the mixture of clay and shells. The sands particle appear angular where they could be seen, but also appear to be eroded and thus it is not fresh angularity, which could be explained by the age of this material.

The clay particles appeared to be well separated by the calcite shells. This separation prevented the clay minerals from forming a continuous matrix. The clay particles being separated explains the low affinity for water as displayed by the material in the laboratory, where it would dry of any moisture content very rapidly. The clay was thought to be a smectite.

At a scale number below 20 μm, the SEM shows views of the calcite material, shells, that could be seen to adopt a preferred orientation. However, this orientation was not consistent in any one direction for the various groups of calcite. Figure 4.37 shows a honeycomb piece of material which is believed to be a sea animal, know as a diatom, which is a calcitic shell fragment. There does not appear to be a difference between the photos at these low scale numbers for the three orientations angles.

The photos indicate that this sample has high porosity. This can be explained by the high content of shell fragments and the voids they create by the way they exist in the sample. The high porosity (or void ratio) matches the laboratory data. The high iron content determined in the sample mineralogy partly explains the soil's high specific gravity, calculated in the laboratory to be 2.90.

A series of four of photos of Syncrude sand are shown in Figure 4.39 after Küpper (1991) The Syncrude sand particle can be seen to be subangular to subrounded with a fairly uniform grain size. The fines mineral in the Syncrude sand appears to be a mix of silt sized particles and clay particles. These particles can be seen mostly at the sand grain contacts The clay appears to form connectors to the sand grains. The grain to grain contacts can be seen in the photos. Detailed analysis of the contacts is given in Law (1991). The fines content of samples in the field taken near the location of these samples ranged from 3.5% to 11.6% passing the #200 sieve.

Test No.	p'c. (kPa)	e	Vs. (m/s)
OS-336-T1-CU	45.5	0.875	122
	144.3	0.871	174
	239.4	0.865	198
	336.3	0.858	231
OS-160-T3-CU	153.7	0.894	181
OS-258-T4-CU	59.0	0.895	123
	258.0	0.859	221
OS-262-T6-CU	66.0	0.802	161
	161.0	0.789	200
	261.0	0.775	237
OS-361-T7-CU	163.0	0.801	201
	261.0	0.793	210
	363.0	0.784	256
OS-335-T9-CU	63.0	0.770	149
	154.0	0.762	193
	252.0	0.754	225
	351.0	0.749	251

Test No.	(p')uss. (kPa)	(e)uss	(Vs)uss. (m/s)	$(\sigma'1)$uss. (kPa)	$(\sigma'3)$uss. (kPa)
OS-160-T3-CU	13.2	0.894	-	22.7	8.4
OS-262-T6-CU	55.0	0.775	150	104.3	30.7
OS-361-T7-CU	48.0	0.784	141	92.6	25.8
OS-358-T8-CU	818.4	0.696	-	1448.7	503.3
OS-335-T9-CU	235.0	0.749	244	430.2	137.4

Table 4.1 Test data obtained during consolidation and at USS for Ottawa sand.

64

Preparation	p'c, (kPa)	e	Vs. (m/s)
MT	100.6	0.814	175
	151.8	0.809	192
	200.8	0.805	212
	250.7	0.802	226
	300.4	0.799	234
	350.5	0.796	245
	400.2	0.794	253
	442.9	0.792	258
	500.7	0.791	267
MT	150.3	0.827	189
	250.7	0.819	207
	350.5	0.813	223
	450.9	0.809	246
	550.6	0.806	258
MT	148.9	0.824	200
	243.9	0.817	228
	349.4	0.812	249
MT	151.2	0.822	202
	254.9	0.816	227
MT	49.1	0.822	138
	148.2	0.813	184
	247.3	0.807	207
	348.8	0.803	224
MT	52.6	0.826	139
	147.7	0.816	184
	247.6	0.808	208
	346.1	0.804	227
WP	55	0.584	181
	105	0.580	235
	156.5	0.578	261
	207.3	0.575	284
	257.2	0.573	300
	306.6	0.570	320
	357.5	0.569	324
	405.1	0.568	333
WP	57.5	0.585	198
	107.1	0.582	231
	173.5	0.578	248
	207.4	0.577	278
	256.7	0.575	299
	307.7	0.574	322
	358.6	0.572	328
	419.1	0.571	336

Table 4.2 Test data obtained during consolidation and at USS for Ottawa sand after
Sasitharan (1994).

Preparation	p'c. (kPa)	e	Vs. (m/s)
WP	52.9	0.666	183
	76.5	0.663	198
	102.1	0.661	221
WP	102.1	0.682	210
	152.4	0.678	236
	202.6	0.675	255
	253.7	0.672	278
	302.7	0.671	293
	354	0.669	306
	404	0.667	308
WP	58.8	0.679	181
	108.3	0.674	222
WP	107.2	0.675	212
	157.2	0.671	226
	207.5	0.667	265
	257.3	0.665	278
	307.8	0.663	282
	407.9	0.659	308

Preparation	(p')uss. (kPa)	(e)uss	(Vs)uss. (m/s)
MT	53.1	0.793	150
MT	55.3	0.793	145
MT	40.7	0.805	125
MT	18.2	0.809	115
MT	48.4	0.804	-
MT	50.2	0.791	-
MT	535	0.758	-

Table 4.2 Continued.

66

Test No	p'c, (kPa)	e	Vs, (m/s)
AS-40-11-CU	40.4	1.269	88
AS-352-12-CU	48.6	1.118	99
	98.5	1.059	125
	154.0	1.005	150
	201.8	0.976	169
	250.8	0.952	185
	300.4	0.932	211
	350.8	0.915	217
AS-146-13-CU	56.0	1.112	109
	102.5	1.062	135
	154.8	1.010	158
AS-96-15-CU	63.3	1.128	106
	105.9	1.074	139
AS-145-16-CU	49.0	1.152	96
	96.3	1.087	126
	149.0	1.039	152
AS-225-17-CU	47.4	1.110	94
	96.3	1.050	125
	140.7	1.006	149
	190.0	0.974	168
	239.0	0.952	183

Test No	(p')uss, (kPa)	(e)uss	(Vs)uss, (m/s)	(σ'1)uss, (kPa)	(σ'3)uss, (kPa)
AS-40-11-CU	18.7	1.269	-	-	-
AS-352-12-CU	121.9	0.915	162	249.7	58.8
AS-146-13-CU	46.9	1.010	112	96.2	22.6
AS-96-15-CU	33.6	1.074	97	68.2	17.2
AS-145-16-CU	60.2	1.039	106	120.4	31.5
AS-225-17-CU	93.3	0.952	129	182.5	50

Table 4.3 Test data obtained during consolidation and at USS for Alaska sand.

Test No.	p'c. (kPa)	e	Vs. (m/s)
SS-339-T1-CU	48.0	0.936	108
	94.8	0.919	134
	154.0	0.904	158
	197.0	0.896	175
	250.0	0.888	189
	297.0	0.883	202
	348.0	0.877	217
SS-336-T2-CU	48.2	0.946	107
	97.5	0.932	131
	143.9	0.921	149
	195.0	0.913	165
	244.4	0.906	177
	294.1	0.900	188
	345.0	0.896	202
SS-249-T3-CU	48.7	0.934	102
	92.8	0.917	128
	142.9	0.904	146
	191.4	0.895	161
	246.3	0.887	198
SS-340-T4-CU	54.6	0.929	109
	98.4	0.922	130
	145.5	0.914	148
	195.1	0.907	169
	242.3	0.901	180
	292.5	0.896	199
	342.5	0.891	211

Table 4.4 Test data obtained during consolidation and at USS for Syncrude sand.

Test No.	p'c. (kPa)	e	Vs, (m/s)
SS-54-T5-CD	51.0	0.909	124
SS-255-T6-CD	53.7	0.930	117
	100.0	0.914	146
	148.6	0.901	162
	201.6	0.892	182
	248.0	0.884	191
SS-350-T7-CD	49.1	0.935	106
	145.2	0.898	155
	246.1	0.883	182
	343.5	0.871	216
SS-437-T8(AP)-CU	54.0	0.792	137
	145.8	0.774	186
	242.9	0.763	215
	342.3	0.755	220
	440.0	0.749	244
SS-453-T9-CD	49.6	0.886	111
	141.5	0.856	158
	242.3	0.840	191
	340.9	0.829	197
	439.8	0.821	217
SS-352-T10-CU	52.2	0.924	118
	145.2	0.897	158
	243.2	0.881	197
	342.3	0.870	224

Test No	(p')uss. (kPa)	(e)uss	(Vs)uss. (m/s)	$(\sigma'1)$uss. (kPa)	$(\sigma'3)$uss. (kPa)
SS-339-T1-CU	11.1	0.877	79	21.6	5.8
SS-336-T2-CU	9.9	0.896	71	20.5	5.1
SS-249-T3-CU	8.4	0.887	65	16.6	4.4
SS-340-T4-CU	6.8	0.891	-	14.4	2.9
SS-54-T5-CD	102.5	0.808	160	192.8	57.3
SS-255-T6-CD	431.3	0.789	243	796.5	248.7
SS-350-T7-CD	607.9	0.779	236	1138.9	342.3
SS-437-T8(AP)-CU	298.5	0.749	221	571.0	162.2
SS-453-T9-CD	779.0	0.724	343	1454.6	441.3
SS-352-T10-CU	31.6	0.870	94	66.2	13.9

Table 4.4 Continued.

C-CORE

Consolidated Undrained, triaxial compression

Air Pluviated

Figure No.	ess	p'uss, (kPa)	quss, (kPa)
9	0.789	49.0	58.8
10	0.786	110.9	132.6
11	0.775	374.5	476.4

UBC

Consolidated Undrained, triaxial compression

Water Pluviated

Test No.	ess	p'uss, (kPa)	quss, (kPa)
CC1	0.874	392.3	288.0
CC5	0.867	868.0	1168.0

UBC

Consolidated Undrained, simple shear

Air Pluviated

Test No.	ess	p'uss, (kPa)	quss, (kPa)
syn01	0.800	56.0	56.8
syn02	0.840	15.3	16.0
syn03	0.850	10.3	13.0
syn04	0.870	8.4	7.2
AP01	0.823	35.7	40.0
AP03	0.804	40.0	45.0
AP10	0.792	22.8	25.0

UBC

Consolidated Undrained, simple shear

Water Pluviated

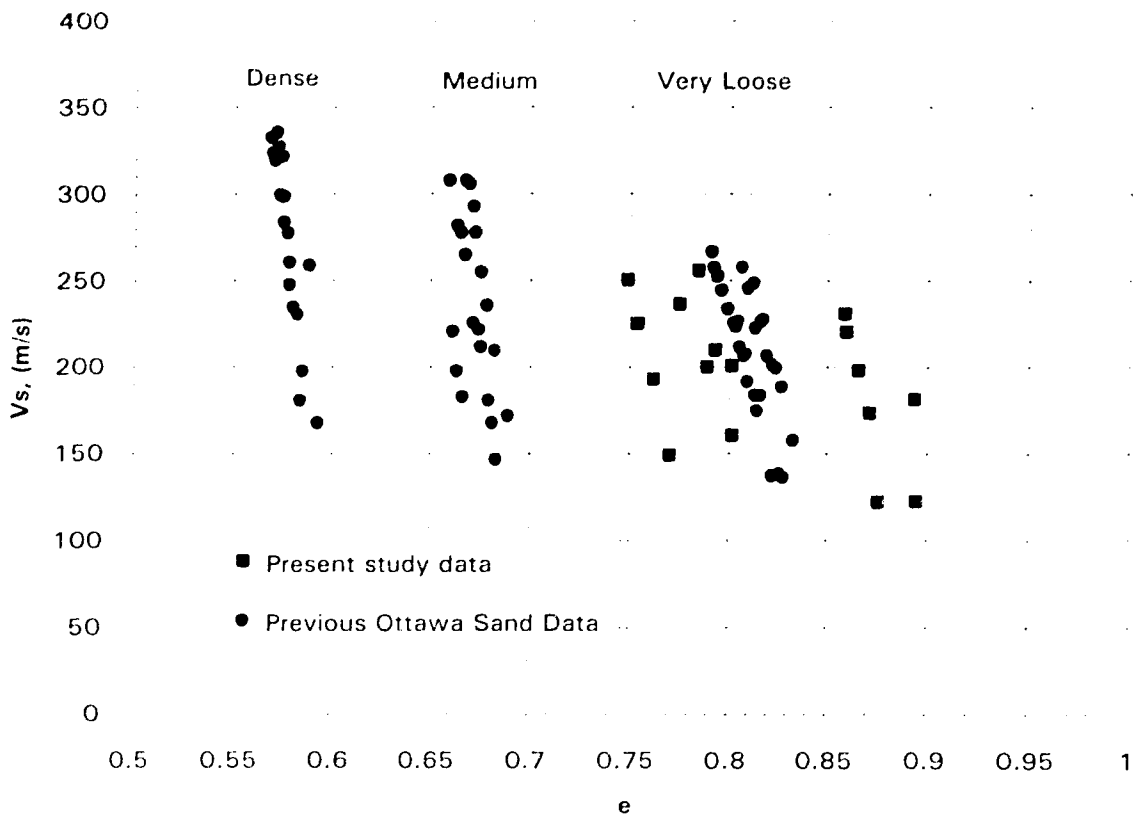| Test No.	ess	p'uss, (kPa)	quss, (kPa)
WP02	0.757	100.2	137.5
WP03	0.792	106.7	154.0

Table 4.5 Syncrude sand USS results from CANLEX (1994)

Figure 4 1 Vs against void ratio for Ottawa sand during consolidation with data from present study and after Sasitharan (1994).
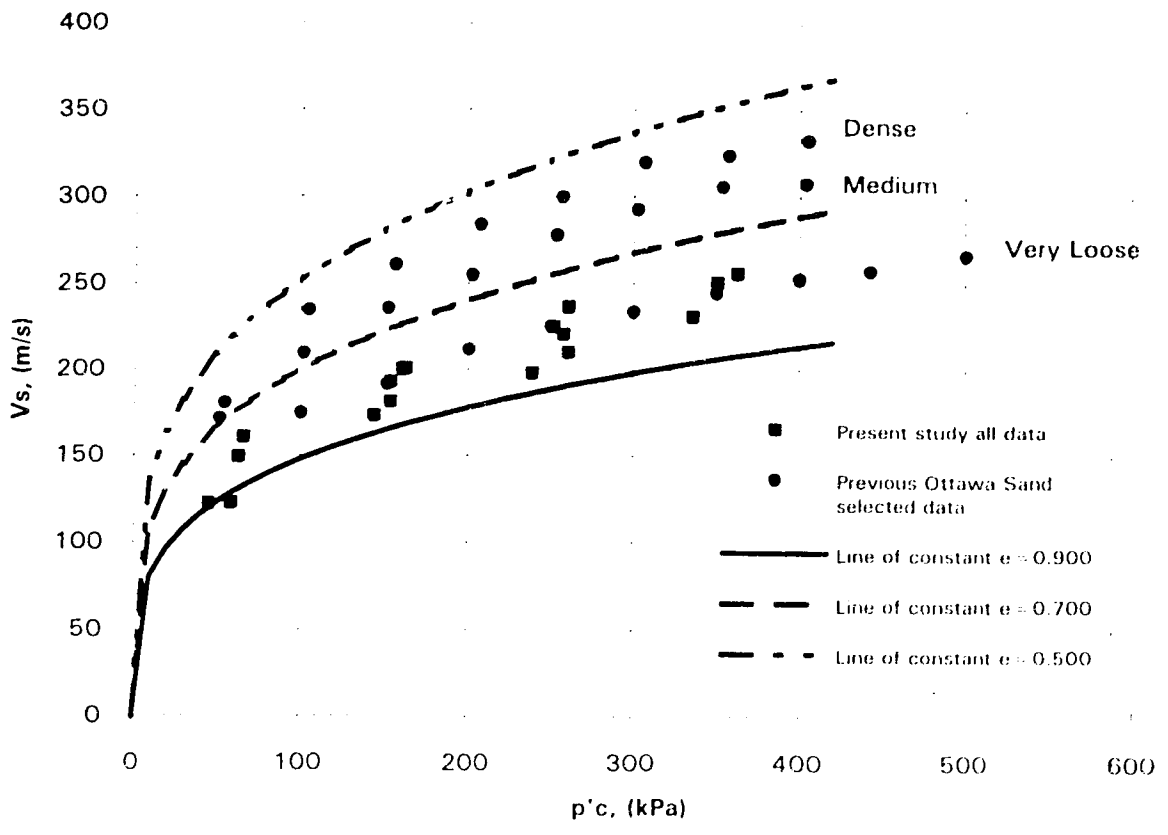
Figure 4.2 Vs against effective consolidation stress for Ottawa sand during consolidation with data from present study and selected data after Sasitharan (1994)
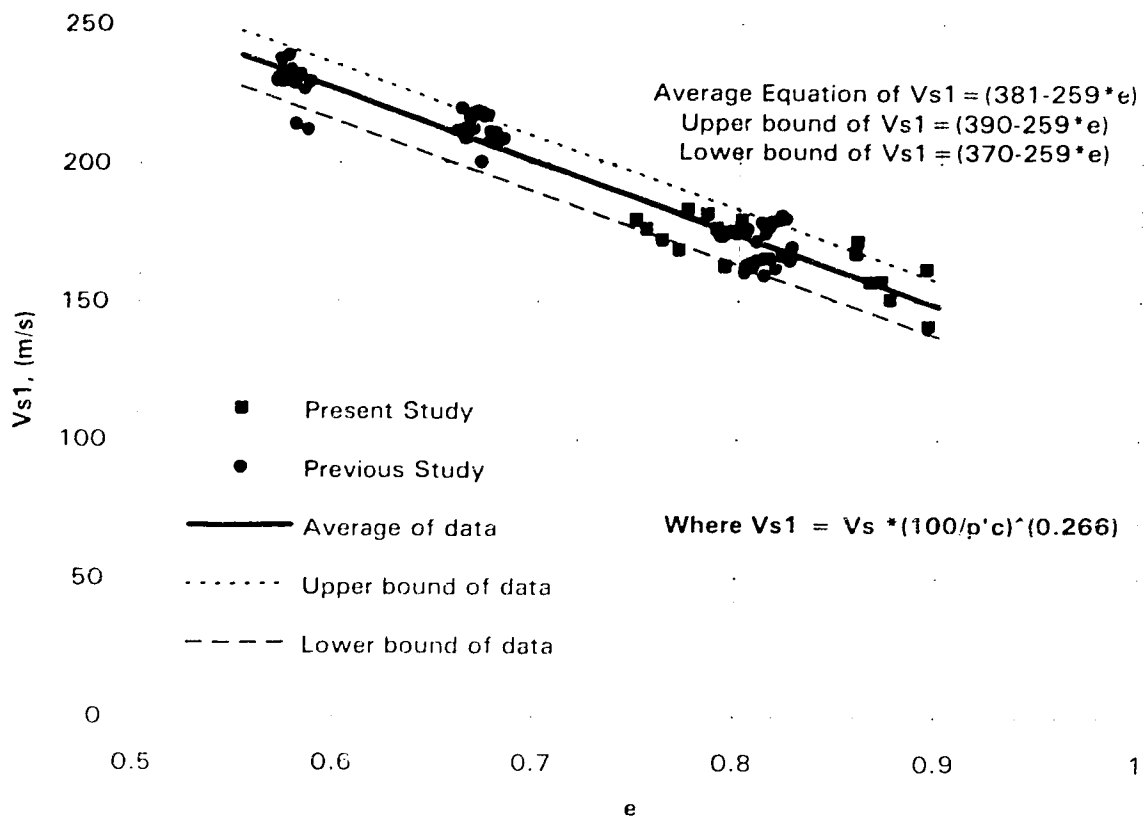
Figure 4.3 Vs1 against void ratio for Ottawa sand during consolidation with data from present study and after Sasitharan (1994) showing average fit as well as upper and lower bound fit.
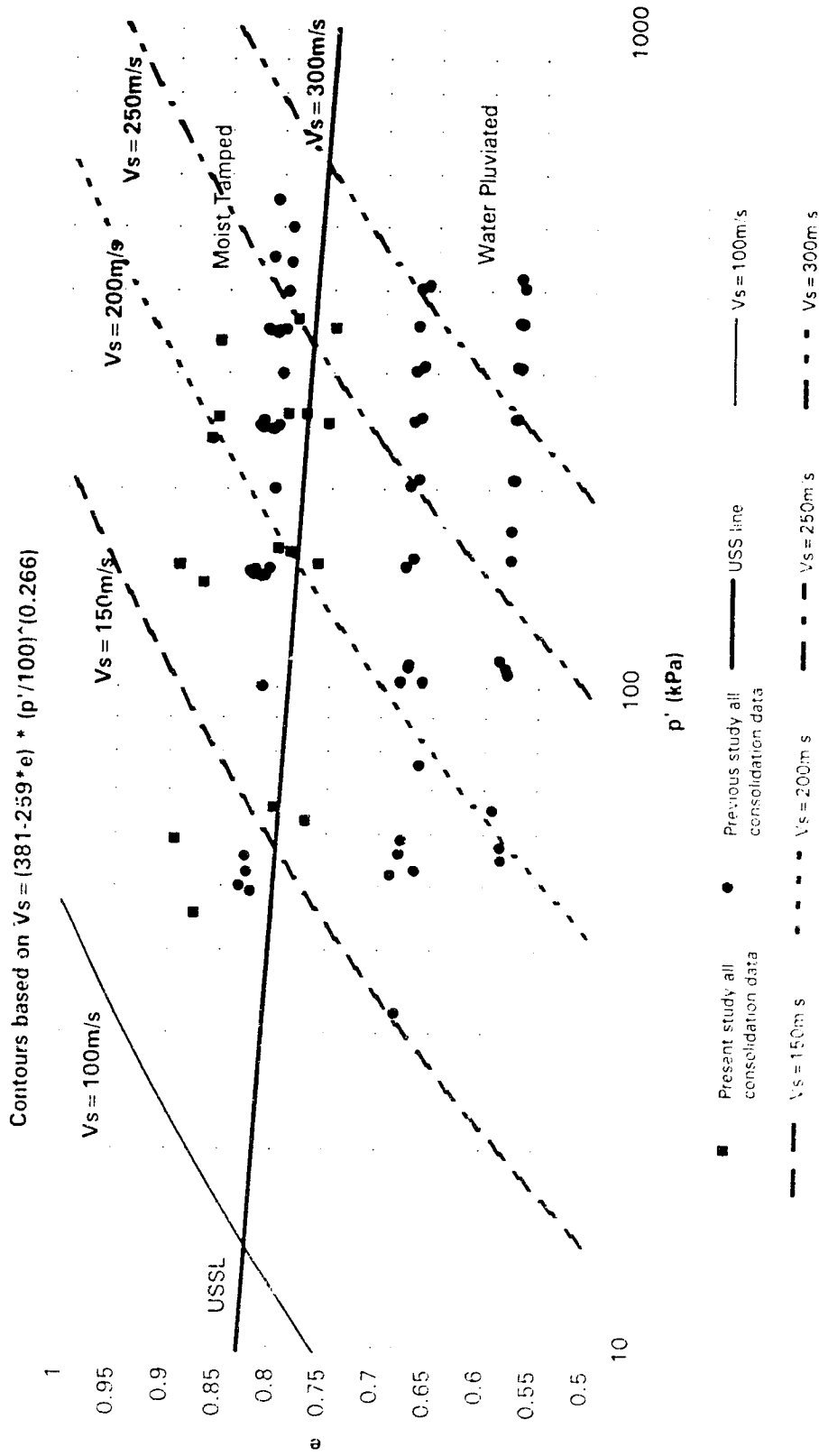
Contours based on Vs = (381-259*e) * (p'/100)^(0.266)

Vs = 100m/s

Vs = 150m/s

Vs = 200m/s

Vs = 250m/s

Vs = 300m/s

Moist Tamped

Water Pluviated

USSL

1

0.95

0.9

0.85

0.8

0.75

0.7

0.65

0.6

0.55

0.5

e

10

100

1000

p' (kPa)

Present study all
consolidation data

Vs = 150m/s

Vs = 200m/s

Previous study all
consolidation data

USS line

Vs = 100m/s

Vs = 250m/s

Vs = 300m/s

Figure 4.4 Consolidation data for Ottawa sand with data from present study and Sasitharan (1994), also showing contours of Vs in m/s.

74
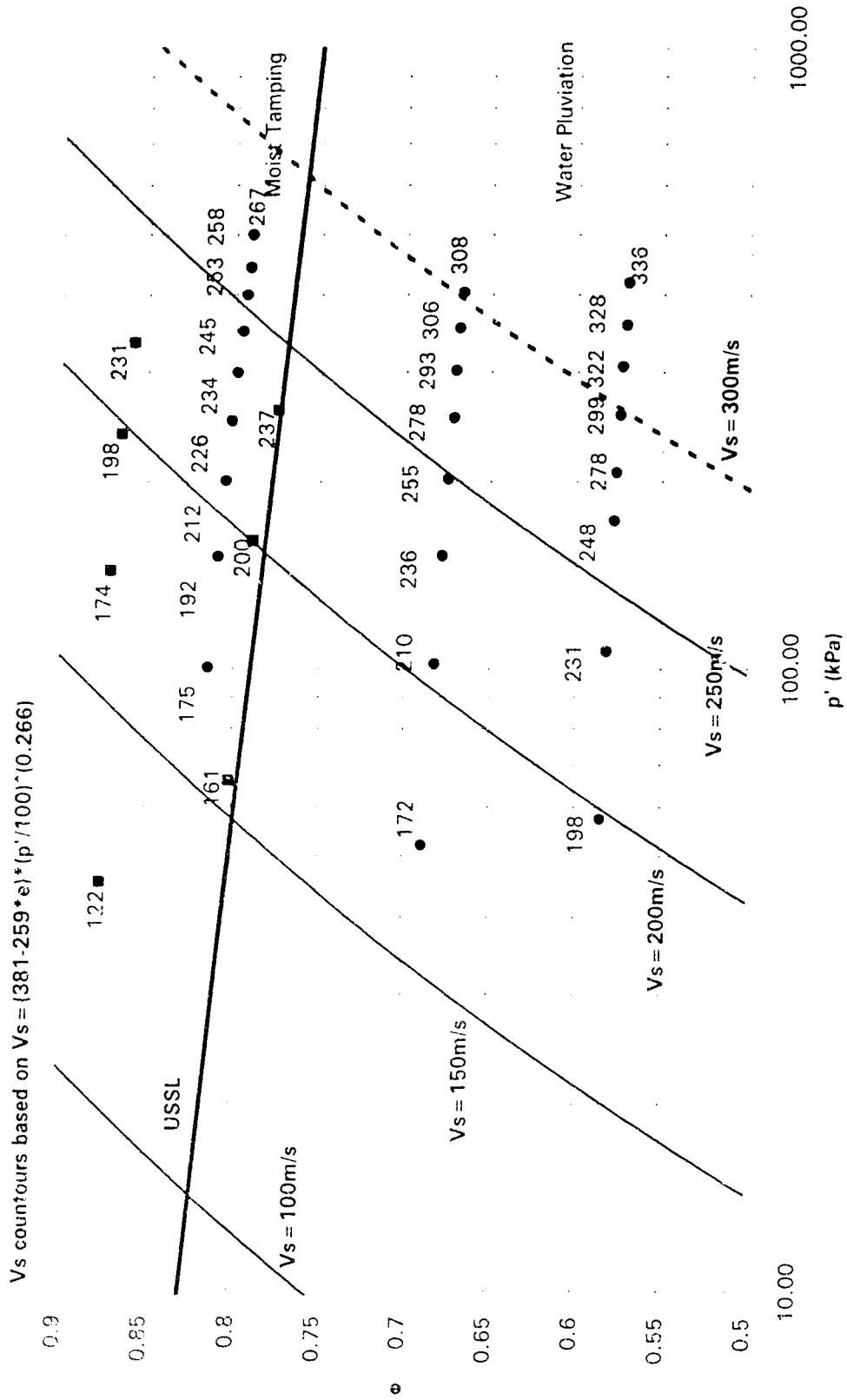
Figure 4.5 p' against void ratio with contours of Vs based on Ottawa sand e-p'-Vs equation showing lab consolidation states marked with measured Vs in m/s.
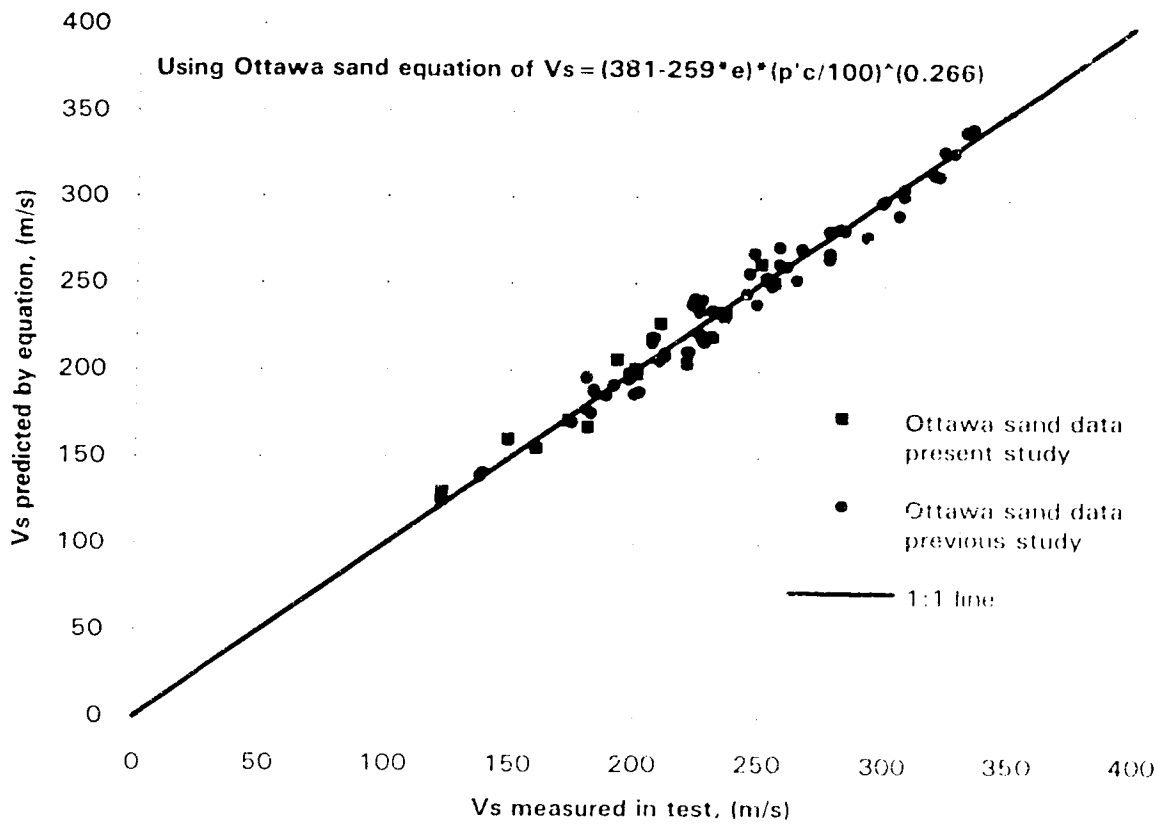
Figure 4   Measured Vs in laboratory against Vs predicted by equation for Ottawa sand during consolidation for data from present study and after Sasitharan (1994)